

See discussions, stats, and author profiles for this publication at: <https://www.researchgate.net/publication/263587284>

Analytical Solution of Free Radical Polymerization: Derivation and Validation

ARTICLE in *MACROMOLECULES* · JULY 2014

Impact Factor: 5.8 · DOI: 10.1021/ma500480z

CITATIONS

7

READS

65

6 AUTHORS, INCLUDING:



Dhiraj Kumar Garg

Shiv Nadar University

12 PUBLICATIONS 49 CITATIONS

SEE PROFILE



Christophe A Serra

University of Strasbourg

104 PUBLICATIONS 1,272 CITATIONS

SEE PROFILE



Yannick Hoarau

University of Strasbourg

69 PUBLICATIONS 354 CITATIONS

SEE PROFILE



Dambarudhar Parida

University of Bordeaux

13 PUBLICATIONS 55 CITATIONS

SEE PROFILE

Analytical Solution of Free Radical Polymerization: Derivation and Validation

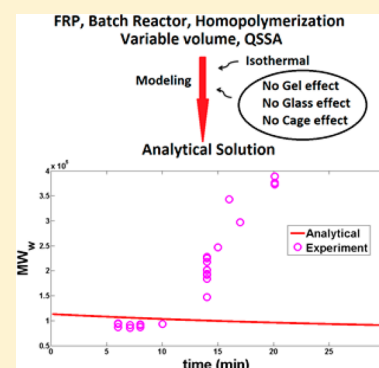
Dhiraj K. Garg,^{†,‡} Christophe A. Serra,^{*,‡} Yannick Hoarau,[†] Dambarudhar Parida,[‡] Michel Bouquey,[‡] and René Muller[‡]

[†]Laboratoire des Sciences de l'Ingénieur, de l'Informatique et de l'Imagerie (ICUBE), Université de Strasbourg (UdS), Strasbourg 67000, France

[‡]Groupe d'Intensification et d'Intégration des Procédés Polymères (G2IP), Institut de Chimie et Procédés pour l'Énergie, l'Environnement et la Santé (ICPEES) – UMR 7515 CNRS, École Européenne de Chimie, Polymères et Matériaux (ECPM), Université de Strasbourg (UdS), Strasbourg 67087, France

S Supporting Information

ABSTRACT: An elegant, simple, and exact analytical solution (AS) was obtained for a large range of elementary steps with practical importance in free radical polymerization. The AS matches excellently with the numerical solution for the four cases of monomer–polymer systems studied ranging from the slowest to the fastest. It works equally well for different initiators, different initiator and monomer concentrations, presence or absence of solvent, various solvent volume fractions, and different temperatures. It also matches quite well with experimental data reported in the literature. This AS is not only in line with previous published solutions but also extends their applicability in a natural way. Overall, the conceptual correctness as well as predictive capabilities of the derived AS are established beyond doubt. This AS has the potential to be used in various practical applications such as model based process control, CFD simulations, and so forth.



INTRODUCTION

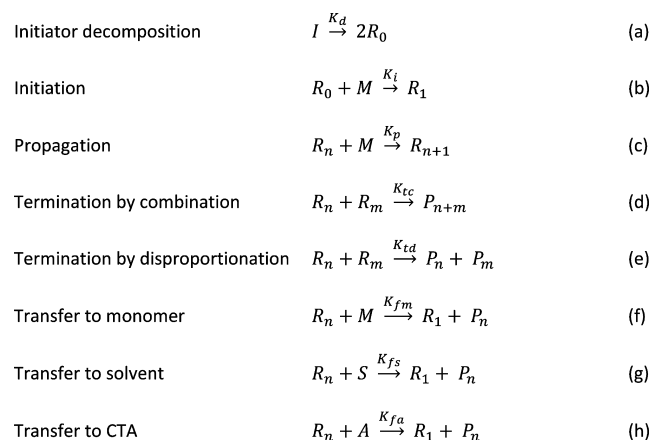
An explicit analytical solution (AS) is always desirable for a given set of mathematical equations. It is especially valuable for mathematical models. Not only does it reduce the effort by generating a final accurate solution in one step, but also it gives a significant insight of the problem. It is also useful in the validation of the formulation of numerical problems by comparing the numerical solution with AS. Free radical polymerization (FRP) is one such problem which is widely simulated,^{1–7} and an AS of its mathematical model will always be helpful.

To obtain any meaningful result from the simulation of any problem, it is necessary that the problem should be modeled properly. Theoretically, the best modeling of any problem is the one which encompasses all the aspects of the problem. But this ideal condition is often not so practical. Indeed, not all aspects of the problems might be understood properly to formulate them mathematically. On the other hand, it might be too computationally exhaustive to include all effects, both minor and major. Thus, it might not be economically feasible in terms of time and resources to obtain any meaningful results. So, several assumptions are made to simplify the problem. Too much simplification also has the adverse effect of losing all the vital aspects of the problem, thus rendering the solution useless. Thus, an adequate simplification of the problem is the one which reduces the unnecessary and insignificant aspects of the problem under the given conditions while still retaining the essence of the problem. The extent of simplification and thus the assumptions

can vary either with the conditions under which the solution is desired or with the level of insight required in the problem.

There are several elementary reaction steps that characterize a real FRP scheme, but any model of FRP includes a minimum of four steps as shown in Scheme 1, namely, (a) initiator

Scheme 1. Kinetic Scheme for Free Radical Polymerization Used in This Work



Received: March 5, 2014

Revised: June 2, 2014

decomposition, (b) initiation, (c) propagation, and (d) termination. Steps (a) and (b) are generally clubbed together with an initiator efficiency factor f , for simplifying modeling. There is one parallel reaction each to step (c) and step (d), namely, transfer to monomer (step (f)) and termination by disproportionation (step (e)), respectively. There are several other competitive reactions to the propagation step, for example, transfer to solvent (g), transfer to chain transfer agent (CTA) (h), and so forth. Many researchers used various combinations of the above-mentioned steps for modeling and matching the numerical results against experimental data with different success.^{1–7} Effect of solvent is also considered to a different extent in the modeling by considering either the reaction steps involving solvent or its dilution effects on species concentration and temperature or both. The kinetic model of FRP considered in this paper has also been used by many researchers^{7,8} and is fairly good and sufficient enough for many practical situations. Not all steps could practically be considered due to the excessively increased level of complexity for deriving an AS.

One of the most sought after solutions for any chemical reaction is the one for ideal batch reactor form. However, a plug flow reactor at different axial positions in continuous flow process is equivalent to a batch reactor varying with time. So any solution obtained for a batch reactor is directly applicable to plug flow reactors and hence to continuous flow reactors. Thus, it is this benchmark against which the efficiency and effectiveness of all other reactors and reactor conditions are tested. To obtain any solution including AS for the ideal batch reactor, the problem has to be formulated under batch reactor conditions. For this, several assumptions have to be made. The mathematical formulation of FRP in its entirety is quite nonlinear. Various chemical and physical variables, for example, kinetic rate coefficients, initiator efficiency, density of various chemical species, and so forth, are functions of temperature, pressure, species concentration, solution density, and viscosity. But to keep the problem manageable, one generally makes certain assumptions and the extent of accuracy of these assumptions depends on the conditions in which they are applied. So, various assumptions are taken to make the problem linear to arrive at any solution including AS.

Several researchers have given empirical, semiempirical or semi-analytical for FRP, and can be found in a complete review.¹⁰ Zhu and Hamielec²¹ have given the AS for initiator and monomer conversion only. Another attempt was made in the past for giving an AS for FRP by Venkateshwaran and Kumar.⁹ However, there are several notable and significant differences between their work and the one presented here. Authors⁹ worked on reaction steps which included only initiation, propagation, termination by combination and disproportionation, as well as transfer to CTA. Their main assumptions are isothermal, homogeneous, constant volume homopolymerization with time invariant kinetic rate coefficients. They did not consider the quasi-steady state assumption (QSSA) for the moments of live polymer chain length distribution of various orders including zeroth (λ_0), the most important one. Using aforementioned assumptions, they had derived the AS for λ_0 . The solution is in terms of infinite series of Bessel equations. Then, they went on to derive the AS for other variables such as monomer concentration, second and third order moments of the living polymer chain length distribution, and zeroth, first, and second order moment of the dead polymer chain length distribution. The AS they obtained is too complicated and lengthy. The solution seems to be very impractical in its application. Besides this, the AS matched quite poorly with numerical solution even for the

isothermal, nongel/glassy situation for which it was originally derived. Furthermore, they had used several assumptions to express the monomer concentration and then came up with a final form. The latter was similar to the one shown by Zhu and Hamielec,²¹ although that work was based on QSSA for the live polymer chain length distribution. Venkateshwaran and Kumar⁹ had also integrated the energy equation for temperature using the same assumption of constant kinetic rate coefficients. This assumption will further be discussed and commented in the Discussion.

Compared to their work, we have extended the set of elementary steps to transfer to monomer and transfer to solvent, similar to the one used by Tefera et al.⁵ The reaction scheme now includes seven major elementary steps, namely, initiator dissociation and initiation, chain propagation, chain transfer to monomer, chain transfer to solvent, chain transfer to CTA, chain termination by combination, and chain termination by disproportionation. It has been derived directly from theoretical kinetics, so it is neither empirical nor semiempirical nor semianalytical. An explicit AS has been obtained for isothermal, variable volume, homogeneous batch reactor conditions for bulk/solution free radical homopolymerization. No gel effect, glass effect, or cage effect is considered for modeling. Four monomer–polymer systems have been considered in this work based on their rate of reaction which varies from slow for one monomer to extremely fast for another. These monomers are styrene (St), methyl methacrylate (MMA), butyl acrylate (BuA), and vinyl acetate (VAc). The AS has also been validated with solvent (solution polymerization) and without solvent (bulk polymerization) conditions. Two different initiators, namely, 2,2'-azobis(2-methylpropionitrile) (AIBN) and benzoyl peroxide (BPO), with their different concentrations have also been used for simulation. Isothermal conditions have been considered with constant temperature varying discretely from 60 to 100 °C. The results have been compared with numerical solution as well as with published experimental data.

Model of FRP for This Work. The various steps considered in this work are shown in Scheme 1.⁵

The mathematical model for this kinetic scheme is based on the moment method which is quite common and is also quite successful in predicting various statistically averaged properties of the polymers. Here we have defined the moments of n th order

$$\lambda_n = \sum_{i=1}^{\infty} i^n R_i \quad (1)$$

$$\mu_n = \sum_{i=1}^{\infty} i^n P_i \quad (2)$$

where λ_n is n th order of moment of live polymer chain length distribution, whereas μ_n is n th order of moment of dead polymer chain length distribution. λ_0 , λ_1 , and λ_2 are zeroth, first, and second order moment, respectively, of live polymer chain length distribution, whereas μ_0 , μ_1 , and μ_2 are zeroth, first, and second order moment, respectively, of dead polymer chain length distribution. Effects of solvent (physical effects through contribution to mixture density and thermal capacity and chemical effects through transfer to solvent process) and variation in reactor volume with reaction are also modeled. The detailed mathematical model⁵ studied in this work is based on the mass balances of the different chemical species in an ideal batch reactor and is given in Appendix A in the Supporting Information.

■ DERIVATION

To derive the AS, the following assumptions were applied to eqs A1–A11 (Appendix A in the Supporting Information).

(1) Only one monomer-polymer system is considered at a time (homopolymerization).

(2) Constant temperature (isothermal condition), so that kinetic rate coefficients and density of monomer and polymer remain constant with respect to temperature.

(3) Uniform mixing (so no spatial variation of concentration thus no effect of diffusion and convection is to be considered).

(4) Constant initiator efficiency f , throughout reaction (no cage effect).

(5) Kinetic rate coefficients are considered to be a function of temperature only (thus no gel and glass effect), and thus, they remain constant during derivation.

(6) Quasi-steady state assumption (QSSA) applied to radical polymer chains number instead of concentration in eqs A6–A8.

(7) Long chain hypothesis for the monomer consumption.

After applying the above-mentioned assumptions, we will take one equation at a time and solve it appropriately. We will be taking limits from time step t_{n-1} to t_n and all other variables values will be evaluated accordingly for the integration. This approach will lead to final derived equations that would be useful for semibatch conditions where conditions can be changed at a given time or for a given time step. This form will also be useful for process control purposes, as the equations can be rearranged for $t_n - t_{n-1} = \Delta t$ form. For a more general form, that is, calculating any variable at a given time t , equations can be evaluated using the limits $t_0 = 0$ and $t_n = t$. The equations can also be used for constant volume conditions.

$$\frac{1}{V_R} \frac{d(IV_R)}{dt} = -K_d I \quad (\text{A1})$$

Initiator Concentration (eq A1). Rearranging and integrating leads to

$$IV_R = \text{Int_const} e^{-K_d t} \quad (3)$$

where Int_const is an integration constant.

Applying limits from time step t_{n-1} to t_n gives

$$\frac{[IV_R]_n}{[IV_R]_{n-1}} = e^{-K_d(t_n - t_{n-1})} \quad (4)$$

Rearranging

$$[I]_n = [I]_{n-1} \frac{[V_R]_{n-1}}{[V_R]_n} e^{-K_d(t_n - t_{n-1})} \quad (5)$$

We will now introduce a new term so-called corrected volume ratio, V_{corr} to account for volume variation which is defined as

$$V_{\text{corr}} = \frac{[V_R]_{n-1}}{[V_R]_n} \quad (6)$$

For constant volume condition,

$$V_{\text{corr}} = 1 \quad (7)$$

Let

$$y_n = e^{-K_d t_n / 2} \quad (8)$$

and

$$\frac{y_n}{y_{n-1}} = e^{-K_d(t_n - t_{n-1})/2} = e^{-K_d \Delta t / 2} = \Delta y, \quad (9)$$

where $\Delta t = (t_n - t_{n-1})$.

Therefore,

$$[I]_n = [I]_{n-1} \frac{[V_R]_{n-1}}{[V_R]_n} e^{-K_d(t_n - t_{n-1})} = [I]_{n-1} V_{\text{corr}} [\Delta y]^2 \quad (10)$$

Applying limits of $t_{n-1} = t_0 = 0$ to $t_n = t$, we have

$$I = I_0 \frac{V_{R0}}{V_R} e^{-K_d t} = I_0 \frac{V_{R0}}{V_R} y^2 \quad (11)$$

where

$$y = e^{-K_d t / 2} \quad (12)$$

Monomer Conversion (eq A3). We are presenting here the final expression of the AS for monomer conversion. For details, please refer to Appendix B in the Supporting Information.

$$[x_M]_n = 1 - [1 - x_M]_{n-1} \exp[-B_{n-1}(1 - \Delta y)] \quad (13)$$

where

$$B_{n-1} = \sqrt{\frac{8f[K_{pr}]^2 I_{n-1}}{K_d K_t}} \quad (14)$$

Applying limits of $t_{n-1} = t_0 = 0$ to $t_n = t$, we have

$$\Delta t = t \text{ and } \Delta y = y \quad (15)$$

$$x_M = 1 - \exp[-B_0(1 - y)] \quad (16)$$

where

$$B_0 = \sqrt{\frac{8f[K_{pr}]^2 I_0}{K_d K_t}} \quad (17)$$

From eq A37 for monomer concentration and eq 13 above, we can derive relationship between monomer concentrations at two different time intervals

$$\begin{aligned} [M]_n &= [M]_{n-1} \frac{[1 - x_M]_n}{[1 - x_M]_{n-1}} \frac{[V_R]_{n-1}}{[V_R]_n} \\ &= [M]_{n-1} \frac{[1 - x_M]_n}{[1 - x_M]_{n-1}} V_{\text{corr}} \\ &= [M]_{n-1} \exp[-B_{n-1}(1 - \Delta y)] V_{\text{corr}} \end{aligned} \quad (18)$$

By integrating eq A2 directly for monomer concentration, we will still get the same equation as above.

Applying limits of $t_{n-1} = t_0 = 0$ to $t_n = t$, we have

$$\begin{aligned} M &= M_0 \frac{\exp[B_0(y - 1)]}{(1 - \epsilon x_M)} \\ &= M_0 \frac{\exp[-B_0(1 - y)]}{(1 - \epsilon x_M)} \\ &= \frac{M_0 V_{R0}}{V_R} \exp[-B_0(1 - y)] \end{aligned} \quad (19)$$

$$-\frac{1}{V_R} \frac{d(SV_R)}{dt} = K_{fs} S \lambda_0 = C_S K_p S \lambda_0 = R_S K_{pr} S \lambda_0 \quad (\text{A4})$$

Transfer to Solvent (eq A4). Integrating similarly as for x_M , we have

$$(SV_R) = \exp[R_S B e^{-K_d t/2}] \quad (20)$$

Applying limits from time step t_{n-1} to t_n , we obtain after rearranging:

$$\begin{aligned} [S]_n &= [S]_{n-1} \exp[-R_S B_{n-1}(1 - \Delta y)] \frac{[V_R]_{n-1}}{[V_R]_n} \\ &= [S]_{n-1} \exp[-R_S B_{n-1}(1 - \Delta y)] V_{\text{corr}} \end{aligned} \quad (21)$$

Applying limits of $t_{n-1} = t_0 = 0$ to $t_n = t$, we have

$$S = S_0 \frac{\exp[-R_S B_0(1 - y)]}{(1 - \varepsilon x_M)} = \frac{S_0 V_{R0}}{V_R} \exp[-R_S B_0(1 - y)] \quad (22)$$

So dividing the above equation with M (eq 19), we have

$$\begin{aligned} \frac{S}{M} &= \frac{S_0}{M_0} \frac{\exp[-R_S B_0(1 - y)]}{\exp[-B_0(1 - y)]} \\ &= \frac{S_0}{M_0} \exp[(1 - R_S)B_0(1 - y)] \end{aligned} \quad (23)$$

Transfer to CTA (eq A5). Similarly for CTA

$$-\frac{1}{V_R} \frac{d(AV_R)}{dt} = K_{fa} A \lambda_0 = C_A K_p A \lambda_0 = R_A K_{pr} A \lambda_0 \quad (A5)$$

Applying limits from time step t_{n-1} to t_n , we have after rearranging

$$\begin{aligned} [A]_n &= [A]_{n-1} \exp[-R_A B_{n-1}(1 - \Delta y)] \frac{[V_R]_{n-1}}{[V_R]_n} \\ &= [A]_{n-1} \exp[-R_A B_{n-1}(1 - \Delta y)] V_{\text{corr}} \end{aligned} \quad (24)$$

Applying limits of $t_{n-1} = t_0 = 0$ to $t_n = t$, we have

$$\begin{aligned} A &= A_0 \frac{\exp[-R_A B_0(1 - y)]}{(1 - \varepsilon x_M)} \\ &= \frac{A_0 V_{R0}}{V_R} \exp[-R_A B_0(1 - y)] \end{aligned} \quad (25)$$

So dividing previous equation with M (eq 19), we have

$$\begin{aligned} \frac{A}{M} &= \frac{A_0}{M_0} \frac{\exp[-R_A B_0(1 - y)]}{\exp[-B_0(1 - y)]} \\ &= \frac{A_0}{M_0} \exp[(1 - R_A)B_0(1 - y)] \end{aligned} \quad (26)$$

Now let

$$L = \frac{(K_p + K_{fm})M\lambda_0}{2fK_d I} = \frac{K_{pr}M\lambda_0}{2fK_d I} \quad (27)$$

At the beginning of n th time step

$$[L]_n = \frac{K_{pr}[M]_n[\lambda_0]_n}{2fK_d[I]_n} \quad (28)$$

$$\begin{aligned} \bar{L} &= \frac{K_{pr}M\lambda_0}{2fK_d I + (K_{fm}M + K_{fs}S + K_{fa}A)\lambda_0} \\ &= \frac{(1 - R_{MM})K_{pr}M\lambda_0}{2fK_d I + (R_{MM} + R_{SM} + R_{AM})K_{pr}M\lambda_0} \\ &= \frac{(1 - R_{MM})K_{pr}M\lambda_0}{2fK_d I + R_p K_{pr}M\lambda_0} \end{aligned} \quad (29)$$

$$\bar{L} = L \left(\frac{1 - R_{MM}}{1 + R_p L} \right) = L \left(\frac{1 - R_M}{1 + R_p L} \right) \quad (30)$$

At the beginning of n th time step

$$[\bar{L}]_n = [L]_n \left(\frac{1 - R_M}{1 + R_p [L]_n} \right) \quad (31)$$

λ_0 , Zeroth Order Moment of Live Polymer Chain Length Distribution (eq A6). By applying QSSA on eq A6, we have

$$\lambda_0 = \sqrt{\frac{2fK_d I}{(K_{tc} + K_{td})}} = \sqrt{\frac{2fK_d I}{K_t}} \quad (32)$$

At the beginning of n th time step

$$[\lambda_0]_n = \sqrt{\frac{2fK_d [I]_n}{K_t}} \quad (33)$$

λ_1 , First Order Moment of Live Polymer Chain Length Distribution (eq A7). By applying QSSA on eq A7, we have

$$\begin{aligned} \lambda_1 &= \left[\frac{2fK_d I + (1 + R_{SM} + R_{AM})K_{pr}M\lambda_0}{K_t \lambda_0 + (R_{MM} + R_{SM} + R_{AM})K_{pr}M} \right] \\ &= \lambda_0 \left[\frac{1 + (1 + R_{SA})L}{1 + R_p L} \right] \\ &= \lambda_0 (\bar{L} + 1) \end{aligned} \quad (34)$$

At the beginning of n th time step

$$[\lambda_1]_n = [\lambda_0]_n ([\bar{L}]_n + 1) \quad (35)$$

λ_2 , Second Order Moment of Live Polymer Chain Length Distribution (eq A8). By applying QSSA on eq A8, we have

$$\begin{aligned} \lambda_2 &= \left[\frac{2fK_d I + (1 + R_{SM} + R_{AM})K_{pr}M\lambda_0 + 2K_{pr}M\lambda_1}{K_t \lambda_0 + (R_{MM} + R_{SM} + R_{AM})K_{pr}M} \right] \\ &= \lambda_1 (2\bar{L} + 1) = \lambda_0 (\bar{L} + 1) (2\bar{L} + 1) \end{aligned} \quad (36)$$

At the beginning of n th time step

$$[\lambda_2]_n = [\lambda_1]_n (2[\bar{L}]_n + 1) = [\lambda_0]_n ([\bar{L}]_n + 1) (2[\bar{L}]_n + 1) \quad (37)$$

when

$$\bar{L} \gg 1 \quad (38)$$

$$\lambda_1 = \lambda_0 \bar{L} \quad (39)$$

$$\lambda_2 = 2\bar{L}\lambda_1 = 2\bar{L}^2\lambda_0 \quad (40)$$

and when $R_p = 0$, that is, chain transfer to monomer (R_{MM}), solvent (R_{SM}), and CTA (R_{AM}) are negligible then $\bar{L} = L$

obtained from eq 30. The above simplifications are commonly used by many researchers, but we have not used them for the derivation to keep all the complexity to the possible extent.

$$\begin{aligned} \frac{1}{V_R} \frac{d(\mu_0 V_R)}{dt} &= (K_{fm}M + K_{fs}S + K_{fa}A)\lambda_0 + \left(K_{td} + \frac{K_{tc}}{2}\right)\lambda_0^2 \\ &= (R_M M + R_S S + R_A A)K_{pr}\lambda_0 + \left(1 - \frac{R_T}{2}\right)K_t\lambda_0^2 \end{aligned} \quad (A9)$$

μ_0 , Zeroth Order Moment of Dead Polymer Chain Length Distribution (eq A9). The AS for this equation is given below. The details of the derivation are presented in Appendix C in the Supporting Information.

$$\begin{aligned} [\mu_0]_n &= [\mu_0]_{n-1}V_{corr} + R_M\{[M]_{n-1}V_{corr} - [M]_n\} \\ &+ \{[S]_{n-1}V_{corr} - [S]_n\} + \{[A]_{n-1}V_{corr} - [A]_n\} \\ &+ \left(1 - \frac{R_T}{2}\right)2f\{[I]_{n-1}V_{corr} - [I]_n\} \end{aligned} \quad (41)$$

Applying limits of $t_{n-1} = t_0 = 0$ to $t_n = t$, we have

$$\begin{aligned} \mu_0 &= R_M \left\{ \frac{M_0 V_{R0}}{V_R} - M \right\} + \left\{ \frac{S_0 V_{R0}}{V_R} - S \right\} \\ &+ \left\{ \frac{A_0 V_{R0}}{V_R} - A \right\} + \left(1 - \frac{R_T}{2}\right)2f \left\{ \frac{I_0 V_{R0}}{V_R} - I \right\} \end{aligned} \quad (42)$$

$$\begin{aligned} \frac{1}{V_R} \frac{d(\mu_1 V_R)}{dt} &= (K_{fm}M + K_{fs}S + K_{fa}A)\lambda_1 + (K_{td} + K_{tc})\lambda_0\lambda_1 \\ \lambda_1 &= (R_M M + R_S S + R_A A)K_{pr}\lambda_1 + K_t\lambda_0\lambda_1 \end{aligned} \quad (A10)$$

μ_1 , First Order Moment of Dead Polymer Chain Length Distribution (eq A10). The AS for the above equation is given below. The detailed derivation is presented in Appendix D in the Supporting Information.

$$\begin{aligned} [\mu_1]_n &= [\mu_1]_{n-1}V_{corr} + \{[M]_{n-1}V_{corr} - [M]_n\} \\ &+ \{[S]_{n-1}V_{corr} - [S]_n\} + \{[A]_{n-1}V_{corr} - [A]_n\} \\ &+ 2f\{[I]_{n-1}V_{corr} - [I]_n\} \end{aligned} \quad (43)$$

Applying limits of $t_{n-1} = t_0 = 0$ to $t_n = t$, we have

$$\begin{aligned} \mu_1 &= \left\{ \frac{M_0 V_{R0}}{V_R} - M \right\} + \left\{ \frac{S_0 V_{R0}}{V_R} - S \right\} + \left\{ \frac{A_0 V_{R0}}{V_R} - A \right\} \\ &+ 2f \left\{ \frac{I_0 V_{R0}}{V_R} - I \right\} \end{aligned} \quad (44)$$

$$\begin{aligned} \frac{1}{V_R} \frac{d(\mu_2 V_R)}{dt} &= (K_{fm}M + K_{fs}S + K_{fa}A)\lambda_2 + (K_{td} + K_{tc})\lambda_0\lambda_2 \\ &+ K_{tc}\lambda_1^2 = (R_M M + R_S S + R_A A)K_{pr}\lambda_2 + K_t\lambda_0\lambda_2 + R_T K_t\lambda_1^2 \end{aligned} \quad (A11)$$

μ_2 , Second Order Moment of Dead Polymer Chain Length Distribution (eq A11). The AS of this equation composed of three cases depending on the values of parameters R_L and P given by following equations:

$$R_L = R_P L \quad (45)$$

$$P = \frac{2}{(R_P L + 1)} + \frac{R_T}{(R_P L + 1)^2} \quad (46)$$

We are presenting here only final expressions for each of the three cases. The detailed derivation is given in Appendix E in the Supporting Information.

Case 1

$$R_L \ll 1 \Rightarrow R_L < 0.1 \Rightarrow R_L + 1 \rightarrow 1 \quad (47)$$

Testing condition for computer code $R_L < 0.1$. This case thus represents the physical situation where transfer processes like chain transfer to monomer, solvent and CTA can be neglected completely. So the termination by combination step represented by R_T becomes the deciding factor.

After applying the above condition to eqs 45 and 46, we have

$$P \approx 2 + R_T \quad (48)$$

The solution for this case is given below.

$$\begin{aligned} [\mu_2]_n &= [\mu_2]_{n-1}V_{corr} + P(1 + R_{SA})^2 D_{n-1} \\ &\times \left[\sum_{m=1}^{\infty} \left[\left(\frac{(C_{n-1})^m}{m \cdot m!} - \frac{(C_{n-1} \cdot \Delta y)^m}{m \cdot m!} \right) \right] - \ln(\Delta y) \right] V_{corr} \\ &+ (2P - 1)(1 + R_{SA})\{[M]_{n-1}V_{corr} - [M]_n\} \\ &+ (P - 1)2f\{[I]_{n-1}V_{corr} - [I]_n\} \end{aligned} \quad (49)$$

where

$$D_{n-1} = \frac{2(K_{pr}[M]_{n-1})^2}{K_t K_d} e^{-C_{n-1}} \quad (50)$$

$$C_{n-1} = 2B_{n-1} \sqrt{\frac{[V_R]_{n-1}}{V_{R0}}} \quad (51)$$

Applying limits of $t_{n-1} = t_0$ to $t_n = t$, we have

$$\begin{aligned} \mu_2 &= P(1 + R_{SA})^2 D_0 \left[\sum_{m=1}^{\infty} \left(\frac{(C_0)^m}{m \cdot m!} - \frac{(C_0 \cdot y)^m}{m \cdot m!} \right) - \ln(y) \right] \\ &\times \frac{V_{R0}}{V_R} + (2P - 1)(1 + R_{SA}) \left\{ \frac{M_0 V_{R0}}{V_R} - M \right\} \\ &+ (P - 1)2f \left\{ \frac{I_0 V_{R0}}{V_R} - I \right\} \end{aligned} \quad (52)$$

The details of various terms and the derivation of the above expressions are given in Appendix E in the Supporting Information.

Case 2

$$R_L \approx O(1) \Rightarrow 10 > R_L \geq 0.1 \Rightarrow R_L + 1 = \text{constant} \quad (53)$$

Test condition $10 > R_L \geq 0.1$. This is a situation where the effects of transfer processes like chain transfer to monomer, solvent and CTA are intermediate in nature and could no longer be neglected. It was found and also shown in the Results section that in this range, the variation in R_L was quite low. Thus, it can be assumed to be constant without introducing significant error. So, instead of replacing R_L with a fixed numerical value, R_L is retained as variable constant. Its value is evaluated at the beginning of each time interval and will remain constant for that time interval. So one can write

$$P = \frac{2}{(R_L + 1)} + \frac{R_T}{(R_L + 1)^2} \quad (54)$$

where P is assumed to be a variable constant. As can be seen, both chain transfer to monomer and termination by combination steps seem to play role in affecting the value of μ_2 .

Its solution would also be similar to the one already obtained in case 1 (eqs 49–52) except that the coefficients would be different and would be evaluated according to eq 54.

Case 3

$$R_L \gg 1 \Rightarrow R_L \geq 10 \Rightarrow R_L + 1 \rightarrow R_L \quad (55)$$

Test condition $R_L \geq 10$. The physical significance of this situation is that the transfer processes like transfers to monomer, solvent, and CTA, are quite significant. Similar to case 2, here also both termination and transfer steps play an important role in influencing μ_2 . So it comes

$$P = \frac{2}{(R_L)} + \frac{R_T}{(R_L)^2} = \frac{2}{(R_p L)} + \frac{R_T}{(R_p L)^2} \quad (56)$$

The AS for case 3 is given below.

$$\begin{aligned} [\mu_2]_n &= [\mu_2]_{n-1} V_{\text{corr}} + \left(\frac{2}{R_p} (1 + R_{SA})^2 - (1 + R_{SA}) \right) \\ &\times \{ [M]_{n-1} V_{\text{corr}} - [M]_n \} + \left(\frac{R_T}{R_p^2} (1 + R_{SA})^2 \right. \\ &\left. + \frac{4}{R_p} (1 + R_{SA}) - 1 \right) 2f \{ [I]_{n-1} V_{\text{corr}} - [I]_n \} \end{aligned} \quad (57)$$

Applying limits of $t_{n-1} = t_0$ to $t_n = t$, we have

$$\begin{aligned} \mu_2 &= \left(\frac{2}{R_p} (1 + R_{SA})^2 - (1 + R_{SA}) \right) \left\{ \frac{M_0 V_{R0}}{V_R} - M \right\} \\ &+ \left(\frac{R_T}{R_p^2} (1 + R_{SA})^2 + \frac{4}{R_p} (1 + R_{SA}) - 1 \right) \times 2f \left\{ \frac{I_0 V_{R0}}{V_R} - I \right\} \end{aligned} \quad (58)$$

This clearly shows that the μ_2 depends only on initiator and monomer concentration when $R_L \gg 1$, that is, when chain transfer processes are quite significant.

$$\rho V_R C_p \frac{dT}{dt} = (-\Delta H_p) K_p M \lambda_0 V_R - U A_H (T - T_{\text{bath}}) \quad (A12)$$

T, Energy Balance (eq A12). We have assumed C_p and $U A_H$ to be constant here which is quite practical assumption in most cases. Rearranging this equation for T , we have

$$\rho V_R C_p \frac{dT}{dt} - U A_H (T - T_{\text{bath}}) = (-\Delta H_p) K_p M \lambda_0 V_R \quad (59)$$

Dividing it by $\rho C_p V_R$, we have

$$\frac{dT}{dt} - \frac{U A_H}{\rho V_R C_p} (T - T_{\text{bath}}) = \frac{(-\Delta H_p)}{\rho V_R C_p} K_p M \lambda_0 V_R \quad (60)$$

Here ρV_R will remain constant by conservation of mass.

Let

$$K1 = \frac{U A_H}{\rho V_R C_p} \quad (61)$$

$$K2 = \frac{(-\Delta H_p)}{\rho V_R C_p} \quad (62)$$

and applying the transformation of variable

$$T' = T - T_{\text{bath}} \quad (63)$$

we have

$$\frac{dT'}{dt} - K1 T' = K2 K_p M \lambda_0 V_R = K2 (1 - R_M) K_{pr} M \lambda_0 V_R \quad (64)$$

This is a linear differential equation in terms of T' , provided that right-hand side variables are not strong function of temperature. So we have

$$\frac{d}{dt} (e^{(-K1t)} T') = e^{(-K1t)} K2 (1 - R_M) K_{pr} M \lambda_0 V_R \quad (65)$$

Integrating, we have

$$\int d(e^{(-K1t)} T') = \int e^{(-K1t)} K2 (1 - R_M) K_{pr} M \lambda_0 V_R dt \quad (66)$$

$$T' = e^{(K1t)} \int e^{(-K1t)} K2 (1 - R_M) K_{pr} M \lambda_0 V_R dt \quad (67)$$

The right-hand equation seems to be integrable. In fact, Venkateshwaran and Kumar⁹ had integrated it in their paper and published the results without much success. From our point of view, this should not be integrable. One of the main reasons is that, to integrate right-hand side, one has to assume that the explicit and implicit kinetic rate coefficients are constant with respect to change in temperature. And the problem is that it is the temperature only that we are integrating on left-hand side. So which temperature the kinetic rate coefficient will correspond to during integration? To keep this effect of temperature on kinetic rate coefficients low, one needs to keep time step small enough so that kinetic rate coefficients can be assumed nearly constant for the temperature change. This will make the problem stiff, and thus, we can say that temperature equation is the source of stiffness for the above-mentioned reason in this system. The detail of the cause of this stiffness is discussed in the Discussion.

Summary of AS in Time Step Format for Variable Volume Condition. Initiator consumption:

$$[I]_n = [I]_{n-1} \frac{[V_R]_{n-1}}{[V_R]_n} e^{-K_d(t_n - t_{n-1})} = [I]_{n-1} V_{\text{corr}} [\Delta y]^2 \quad (10)$$

where

$$y_n = e^{-K_d t_n / 2} \quad (8)$$

and

$$\frac{y_n}{y_{n-1}} = e^{-K_d(t_n - t_{n-1})/2} = e^{-K_d \Delta t / 2} = \Delta y, \quad (9)$$

where $\Delta t = (t_n - t_{n-1})$.

$$V_{\text{corr}} = \frac{[V_R]_{n-1}}{[V_R]_n} \quad (6)$$

Monomer conversion:

$$[x_M]_n = 1 - [1 - x_M]_{n-1} \exp[-B_{n-1}(1 - \Delta y)] \quad (13)$$

where

$$B_{n-1} = \sqrt{\frac{8f[K_{pr}]^2 I_{n-1}}{K_d K_t}} \quad (14)$$

Monomer consumption:

$$\begin{aligned} [M]_n &= [M]_{n-1} \frac{[1 - x_{M,n}]}{[1 - x_{M,n-1}]} V_{corr} \\ &= [M]_{n-1} \exp[-B_{n-1}(1 - \Delta y)] V_{corr} \end{aligned} \quad (18)$$

Transfer to solvent:

$$[S]_n = [S]_{n-1} \exp[-R_S B_{n-1}(1 - \Delta y)] V_{corr} \quad (21)$$

Transfer to CTA:

$$[A]_n = [A]_{n-1} \exp[-R_A B_{n-1}(1 - \Delta y)] V_{corr} \quad (24)$$

Zeroth order moment of live polymer chain length distribution (QSSA):

$$[\lambda_0]_n = \sqrt{\frac{2fK_d[I]_n}{K_t}} \quad (33)$$

First order moment of live polymer chain length distribution (QSSA):

$$[\lambda_1]_n = [\lambda_0]_n ([\bar{L}]_n + 1) \quad (35)$$

Second order moment of live polymer chain length distribution (QSSA):

$$[\lambda_2]_n = [\lambda_1]_n (2[\bar{L}]_n + 1) = [\lambda_0]_n ([\bar{L}]_n + 1)(2[\bar{L}]_n + 1) \quad (37)$$

Zeroth order moment of dead polymer chain length distribution:

$$\begin{aligned} [\mu_0]_n &= [\mu_0]_{n-1} V_{corr} + R_M \{[M]_{n-1} V_{corr} - [M]_n\} \\ &\quad + \{[S]_{n-1} V_{corr} - [S]_n\} + \{[A]_{n-1} V_{corr} - [A]_n\} \\ &\quad + \left(1 - \frac{R_T}{2}\right) 2f \{[I]_{n-1} V_{corr} - [I]_n\} \end{aligned} \quad (41)$$

First order moment of dead polymer chain length distribution:

$$\begin{aligned} [\mu_1]_n &= [\mu_1]_{n-1} V_{corr} + \{[M]_{n-1} V_{corr} - [M]_n\} \\ &\quad + \{[S]_{n-1} V_{corr} - [S]_n\} + \{[A]_{n-1} V_{corr} - [A]_n\} \\ &\quad + 2f \{[I]_{n-1} V_{corr} - [I]_n\} \end{aligned} \quad (43)$$

Second order moment of dead polymer chain length distribution:

Case 1

$$R_L \ll 1 \Rightarrow R_L < 0.1 \Rightarrow R_L + 1 \rightarrow 1 \quad (47)$$

$$P \approx 2 + R_T \quad (48)$$

$$\begin{aligned} [\mu_2]_n &= [\mu_2]_{n-1} V_{corr} + P(1 + R_{SA})^2 D_{n-1} \\ &\quad \times \left[\sum_{m=1}^{\infty} \left[\left(\frac{(C_{n-1})^m}{m \cdot m!} - \frac{(C_{n-1} \Delta y)^m}{m \cdot m!} \right) \right] - \ln(\Delta y) \right] \\ &\quad \times V_{corr} + (2P - 1)(1 + R_{SA}) \{[M]_{n-1} V_{corr} \\ &\quad - [M]_n\} + (P - 1) 2f \{[I]_{n-1} V_{corr} - [I]_n\} \end{aligned} \quad (49)$$

where

$$D_{n-1} = \frac{2(K_{pr}[M]_{n-1})^2}{K_t K_d} e^{-C_{n-1}} \quad (50)$$

$$C_{n-1} = 2B_{n-1} \sqrt{\frac{[V_R]_{n-1}}{V_{R0}}} \quad (51)$$

Case 2

$$R_L \approx O(1) \Rightarrow 10 > R_L \geq 0.1 \Rightarrow R_L + 1 = \text{constant} \quad (53)$$

$$P = \frac{2}{(R_L + 1)} + \frac{R_T}{(R_L + 1)^2} \quad (54)$$

$$\begin{aligned} [\mu_2]_n &= [\mu_2]_{n-1} V_{corr} + P(1 + R_{SA})^2 D_{n-1} \\ &\quad \times \left[\sum_{m=1}^{\infty} \left[\left(\frac{(C_{n-1})^m}{m \cdot m!} - \frac{(C_{n-1} \Delta y)^m}{m \cdot m!} \right) \right] - \ln(\Delta y) \right] \times V_{corr} \\ &\quad + (2P - 1)(1 + R_{SA}) \{[M]_{n-1} V_{corr} - [M]_n\} \\ &\quad + (P - 1) 2f \{[I]_{n-1} V_{corr} - [I]_n\} \end{aligned} \quad (49)$$

Case 3

$$R_L \gg 1 \Rightarrow R_L \geq 10 \Rightarrow R_L + 1 \rightarrow R_L \quad (55)$$

$$\begin{aligned} [\mu_2]_n &= [\mu_2]_{n-1} V_{corr} + \left(\frac{2}{R_p} (1 + R_{SA})^2 - (1 + R_{SA}) \right) \\ &\quad \times \{[M]_{n-1} V_{corr} - [M]_n\} + \left(\frac{R_T}{R_p^2} (1 + R_{SA})^2 \right. \\ &\quad \left. + \frac{4}{R_p} (1 + R_{SA}) - 1 \right) 2f \{[I]_{n-1} V_{corr} - [I]_n\} \end{aligned} \quad (57)$$

where

$$[L]_n = \frac{K_{pr}[M]_n [\lambda_0]_n}{2fK_d[I]_n} \quad (28)$$

$$[\bar{L}]_n = [L]_n \left(\frac{1 - R_M}{1 + R_p[L]_n} \right) \quad (31)$$

$$R_L = R_p L \quad (45)$$

$$MW_n = \frac{\lambda_1 + \mu_1}{\lambda_0 + \mu_0} MW_M \approx \frac{\mu_1}{\mu_0} MW_M \quad (A14)$$

$$MW_w = \frac{\lambda_2 + \mu_2}{\lambda_1 + \mu_1} MW_M \approx \frac{\mu_2}{\mu_1} MW_M \quad (A15)$$

$$PDI = \frac{MW_w}{MW_n} = \frac{(\lambda_2 + \mu_2)(\lambda_0 + \mu_0)}{(\lambda_1 + \mu_1)^2} \approx \frac{(\mu_2 \mu_0)}{(\mu_1)^2} \quad (A16)$$

$$K_t = K_{tc} + K_{td} \quad (A17)$$

$$K_{pr} = K_p + K_{fm} = (1 + C_M) K_p \quad (A18)$$

$$C_M = \frac{K_{fm}}{K_p} \quad (A19)$$

$$C_S = \frac{K_{fs}}{K_p} \quad (A20)$$

$$C_A = \frac{K_{fa}}{K_p} \quad (A21)$$

$$C_T = \frac{K_{td}}{K_{tc}} \quad (A22)$$

$$R_T = \frac{K_{tc}}{K_{tc} + K_{td}} = \frac{K_{tc}}{K_t} = \frac{1}{1 + C_T} \quad (A23)$$

$$R_M = R_{MM} = \frac{K_{fm}}{K_p + K_{fm}} = \frac{K_{fm}}{K_{pr}} = \frac{C_M}{1 + C_M} \quad (A24)$$

$$R_S = \frac{C_S}{1 + C_M} = \frac{K_{fs}}{K_{pr}} \quad (A25)$$

$$R_{SM} = \frac{C_S}{1 + C_M} \frac{S}{M} = R_S \frac{S}{M} \quad (A26)$$

$$R_A = \frac{C_A}{1 + C_M} = \frac{K_{fa}}{K_{pr}} \quad (A27)$$

$$R_{AM} = \frac{C_A}{1 + C_M} \frac{A}{M} = R_A \frac{A}{M} \quad (A28)$$

$$R_P = R_{MM} + R_{SM} + R_{AM} = R_{MM} + R_{SA} \quad (A29)$$

$$R_{SA} = R_{SM} + R_{AM} \quad (A30)$$

$$\rho = \rho_M \Phi_M + \rho_P \Phi_P + \rho_S \Phi_S \quad (A31)$$

$$C_P = C_{P_M} \Phi_M + C_{P_P} \Phi_P + C_{P_S} \Phi_S \quad (A32)$$

$$\Phi_M = \frac{(1 - x_M)}{(1 - \varepsilon_0 x_M + \beta)} = \frac{(1 - x_M)}{(1 + \beta)(1 - \varepsilon x_M)} \quad (A33)$$

$$\Phi_P = \frac{x_M(1 - \varepsilon)}{(1 - \varepsilon_0 x_M + \beta)} = \frac{x_M(1 - \varepsilon(1 + \beta))}{(1 + \beta)(1 - \varepsilon x_M)} \quad (A34)$$

$$\Phi_S = \frac{\beta}{(1 - \varepsilon_0 x_M + \beta)} = \frac{\beta}{(1 + \beta)(1 - \varepsilon x_M)} \quad (A35)$$

$$V_R = V_{R0}(1 - \varepsilon x_M) \quad (A36)$$

$$M = M_0 \frac{(1 - x_M)}{(1 - \varepsilon x_M)} \quad (A37)$$

$$\varepsilon = \frac{\varepsilon_0}{1 + \beta} \quad (A38)$$

$$\varepsilon_0 = \frac{(\rho_P - \rho_M)}{\rho_P} = 1 - \frac{\rho_M}{\rho_P} \quad (A39)$$

$$\beta = \frac{f_s}{(1 - f_s)} \quad (A40)$$

The summary of AS at any time t for constant volume condition is given in Appendix F in the Supporting Information.

Methodology Adopted. The complete set of eqs A1–A40 in Appendix A of the Supporting Information is named as

FRP_Full model in this study. Many researchers apply quasi-steady state assumption (QSSA)⁷ to the living polymer chain length distributions. Such a model is obtained by applying QSSA to eqs A6–A8 to obtain eqs 32–37 and will be further named as FRP_QSSA. Thus, FRP_QSSA contains all equations as FRP_Full except for eqs A6–A8 which are replaced by eqs 32–37. FRP_QSSA is quite suitable and sufficient for many practical situations of conversions below gel effect where assumption of QSSA is well justified.

The AS was obtained from FRP_QSSA for very simplistic and ideal case, that is, fully mixed, isothermal batch reactor. This removed a lot of complexities and nonlinearity in this mathematical model which helped in obtaining the AS. Theoretically, the solution is strictly valid until the gel effect sets in, after which the assumptions for obtaining AS are not valid.

This solution was validated under similar conditions against numerical solution of the FRP_Full and FRP_QSSA. Matlab R2008a was used for numerical integration and solving AS and postprocessing of the results. Since only isothermal condition was simulated, temperature equation was not required to be solved. As mentioned earlier and will also be presented in detail in the Discussion, the source of stiffness in this model without gel effect comes from temperature equation. So, only nonstiff solver was required for isothermal conditions. Therefore, inbuilt solver of Matlab R2008a - ode23 was used for both FRP_Full and FRP_QSSA.

The simulation results from all the three models, namely, FRP_QSSA, FRP_Full, and Analytical were simultaneously plotted on each graph. FRP_QSSA was represented by green line, FRP_Full by blue line, and Analytical by red line. The experimental data was also plotted in the relevant graphs whenever available and were represented by round circles to signify their discrete nature. Sometimes multiple experimental values for the same given time were found in the literature. So the whole data was plotted without any selection or averaging.

The AS was validated first for isothermal, bulk polymerization with no transfer process case. The theoretical validation by predicting PDI for two different cases of C_T ratio was also done. Then the case of solution polymerization was taken up. After this, the three cases for μ_2 were taken up and had shown how good the AS matches with numerical solution under those conditions. The kinetic and physical data used to simulate above conditions were related to MMA. But the variation in C_T and other parameters like solvent fraction and various transfer kinetic rate coefficients were varied in general manner. This helped to draw general results rather than specific to some monomer. This AS was then finally validated by comparing the results for four monomer-polymer systems, namely, St/PS, MMA/PMMA, BuA/PBuA, and VAc/PVAc. Two initiators AIBN and BPO with varying concentrations were also taken. Toluene was also used as solvent in relevant cases. The data for their various kinetic rate coefficients, physical properties, and so forth were taken from published literature^{3,11–20} and are presented in Table 1. The other experimental data on MW_n , MW_w , and PDI were also used whenever available.

RESULTS

In Figure 1, AS is confronted with a numerical solution for the simplest case of negligible transfer process in bulk isothermal polymerization. As can be seen, the AS matches excellently with numerical solution for all the variables.

The AS must also predict the theoretical results well to prove its validity. When $C_T \ll 1$, that is, when K_{td} is much smaller than K_{tc} , the PDI should be 1.5. When the condition is reverse, then

Table 1. Physical and Chemical Properties of Various Chemical Species under Study

	MMA (ref 13)	styrene (ref 12)
MW (g/mol)	100.13	104.14
ρ_M (g/cm ³)	$0.968-1.225 \times 10^{-3}(T-293.15)$	$0.9236-0.887 \times 10^{-3}(T-273.15)$
ρ_P (g/cm ³)	$1.212-8.45 \times 10^{-4}(T-273.15)$	$1.0855-6.05 \times 10^{-4}(T-273.15)$
K_p (l/mol/min)	$2.95 \times 10^7 \exp(-4353/RT)$	$6.54 \times 10^{-8} \exp(-7051/RT)$
K_{fm} (l/mol/min)	$2.797 \times 10^{11} \exp(-18233/RT)$	$1.38 \times 10^8 \exp(-12670/RT)$
K_t (l/mol/min)	$5.88 \times 10^9 \exp(-701/RT)$	$7.53 \times 10^{10} \exp(-1677/RT)$
$K_{td}/K_{tc} = C_T$	$2.5278 \times 10^3 \exp(-4090/RT)$	0
	BuA (ref 13)	VAc (ref 13)
MW (g/mol)	128.17	86.09
ρ_M (g/cm ³)	$0.9255-1.075 \times 10^{-3}(T-273.15)$	$0.9584-1.3276 \times 10^{-3}(T-293.15)$
ρ_P (g/cm ³)	$1.085-6.05 \times 10^{-4}(T-273.15)$	$1.211-8.496 \times 10^{-4}(T-273.15)$
K_p (l/mol/min)	$1.08 \times 10^9 \exp(-4156/RT)$	$4.2 \times 10^9 \exp(-6300/RT)$
K_{fm} (l/mol/min)	$1.74 \times 10^7 \exp(-7786/RT)$	$1.0206 \times 10^6 \exp(-6300/RT)$
K_t (l/mol/min)	$2.6 \times 10^{12} \exp(-4885/RT)$	$1.62 \times 10^{12} \exp(-2800/RT)$
$K_{td}/K_{tc} = C_T$	0	0
	AIBN (ref 11)	BPO (ref 15)
K_d (1/min)	$6.32 \times 10^{16} \exp(-30\,660/RT)$	$1.69 \times 10^{14} \exp(-25\,383/RT)$
		toluene (ref 3, 20)
MW (g/mol)		92.13
ρ_s (g/cm ³)		$0.883-9 \times 10^{-4}(T-273.15)$

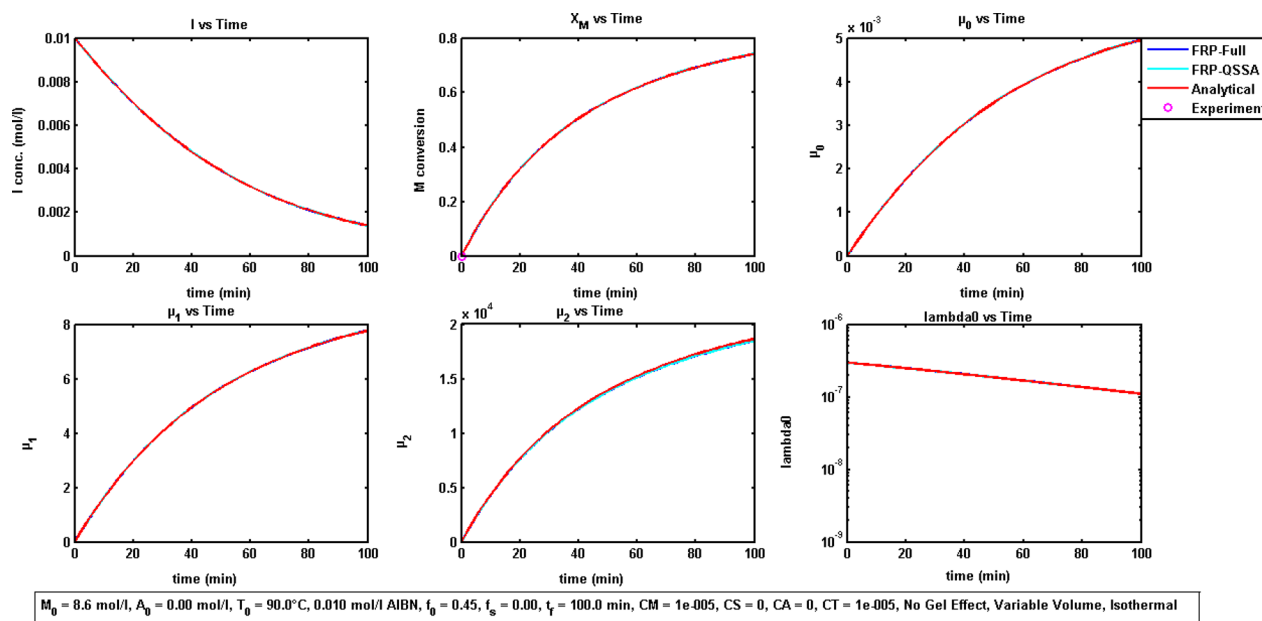


Figure 1. Comparison between AS and numerical solution for general case of isothermal bulk polymerization and negligible transfer processes.

PDI should be 2. So C_T is taken to be equal to either 10^{-5} or 10^5 for simulating these two situations respectively. As can be seen in Figure 2, the PDI is calculated to be 1.5 for $C_T = 10^{-5}$. For $C_T = 10^5$, the PDI is calculated to be 2 as shown in Figure 3, which is same as predicted for the conditions mentioned above. Besides this, despite having similar conversion, decrease in MW_n and MW_w for later case compared to former can easily be observed. This is as per theoretical prediction.

As can be seen in Figure 4, the graphs for λ_0 , λ_1 , and λ_2 as calculated by FRP_Full, FRP_QSSA, and AS match exactly, proving the assumption of QSSA under the given situation.

Now, Figure 5 shows the validation of AS against numerical solution for 30% solvent polymerization with negligible transfer processes. This validates the AS for solution polymerization condition. Again, the matching is excellent with numerical solution.

Now, the 3 cases for μ_2 as obtained in AS are shown in Figures 6–8. Individual cases of AS are evaluated only for transfer to monomer. The results of individual cases are compared with numerical solution for more clarity. As can be seen, individual cases differ significantly from the numerical solution depending upon the value of R_L . Only the one which lies in the range of the R_L value used matches with the numerical solution and is selected for further calculation of MW_w and PDI. This clearly proves the importance of AS from practical point of view. This also proves why it is so difficult to design empirical or semitheoretical formulation for predicting MW_w under various conditions since R_L can have very different values depending on operating conditions (e.g., polymerization time) and monomer–polymer system.

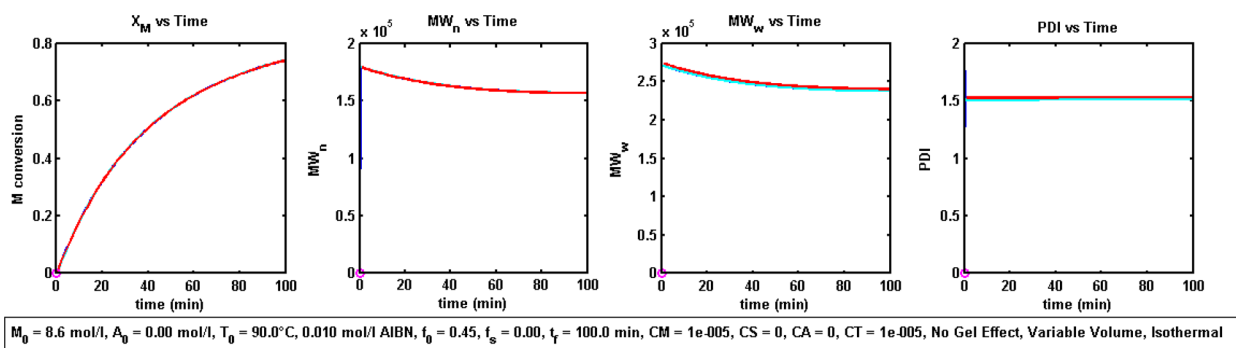


Figure 2. PDI prediction for $C_T = 10^{-5}$ for general case of isothermal bulk polymerization with negligible transfer processes.

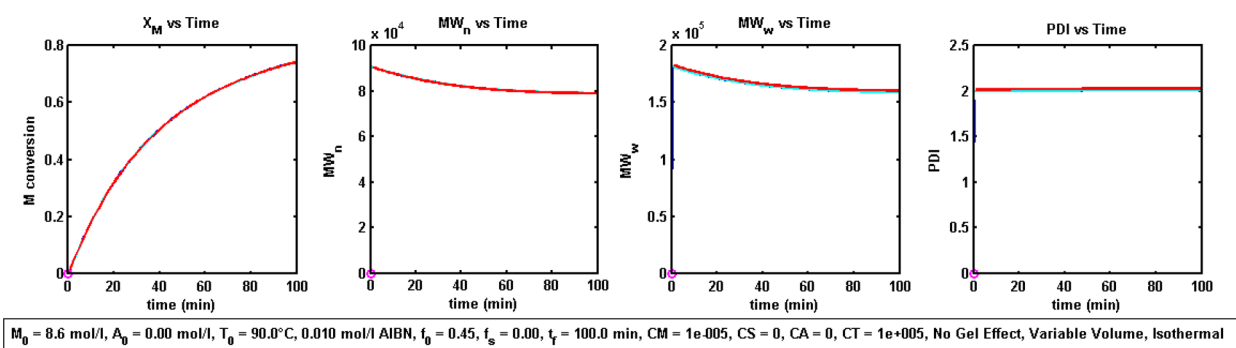


Figure 3. PDI prediction for $C_T = 10^5$ for general case of isothermal bulk polymerization with negligible transfer processes.

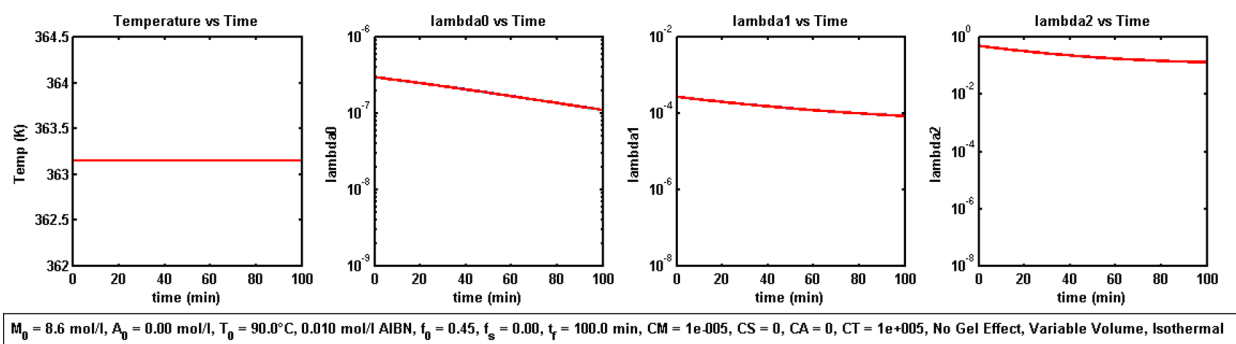


Figure 4. Comparison of λ_0 , λ_1 , and λ_2 as calculated by FRP_Full, FRP_QSSA and AS.

As can be seen for case 2, the value of R_L is varying throughout the time of reaction but the variation is not much. This justifies the assumption of taking R_L constant for this case. Besides this, for time step manner, R_L can be evaluated for each time step for increasing the accuracy of solution instead of choosing the fixed value obtained at $t = 0$.

It is also found that R_L increases by increasing C_M . As a result, μ_2 decreases while shifting from case 1 to case 2 and then to case 3. It is noteworthy that PDI increases and tends to 2 despite C_T being quite less when transfer processes are significant. The latter may include just transfer to monomer as shown in Figures 6–8 or may also include transfer to solvent (C_S) and transfer to CTA (C_A) as shown in Figure 9.

One can also observe the discrepancy between the results for μ_2 selected in Figure 9. It shows that case 2 matches well with numerical solution instead of case 3 which was selected accordingly to our aforementioned criteria (eqs D4, E19, and E25, Supporting Information). This is due to the value of R_L . It was found in our study that case 2 and case 3 overlaps from $R_L = 10$ to 50 and case 1 and case 2 overlaps from $R_L = 0.1$ to 0.05.

So we can only say that the range selected for R_L is good for general conditions. But it can be chosen selectively for individual cases for increasing the quality of results of predictions using AS. Besides, this discrepancy between the AS and numerical solution for case 3 in Figure 9 is also due to assumption of constant R_p taken for obtaining solution for case 3. This also proves that the assumption is quite good and thus justifies itself. To improve the calculations for time step manner, just like R_L , R_{SA} can also be calculated at the beginning of each time step instead of taking constant value calculated at $t = 0$.

Now AS is to be confronted with experimental data. For this, four monomers (St, MMA, BuA, and VAc) are considered. The validation is done under various conditions of different temperatures, initiators, and their different concentrations and solvent fractions. Numerical and analytical solution is also validated against the experimental data for conversion vs time and also for MW_n , MW_w , and PDI wherever data is available.

As can be seen in Figure 10, AS along with numerical solution matches quite well with the experimental data for the conditions before gel effect. In Figure 10, for $T = 80^\circ\text{C}$, it matches well until gel effect sets in, but for $T = 100^\circ\text{C}$, it matches throughout the

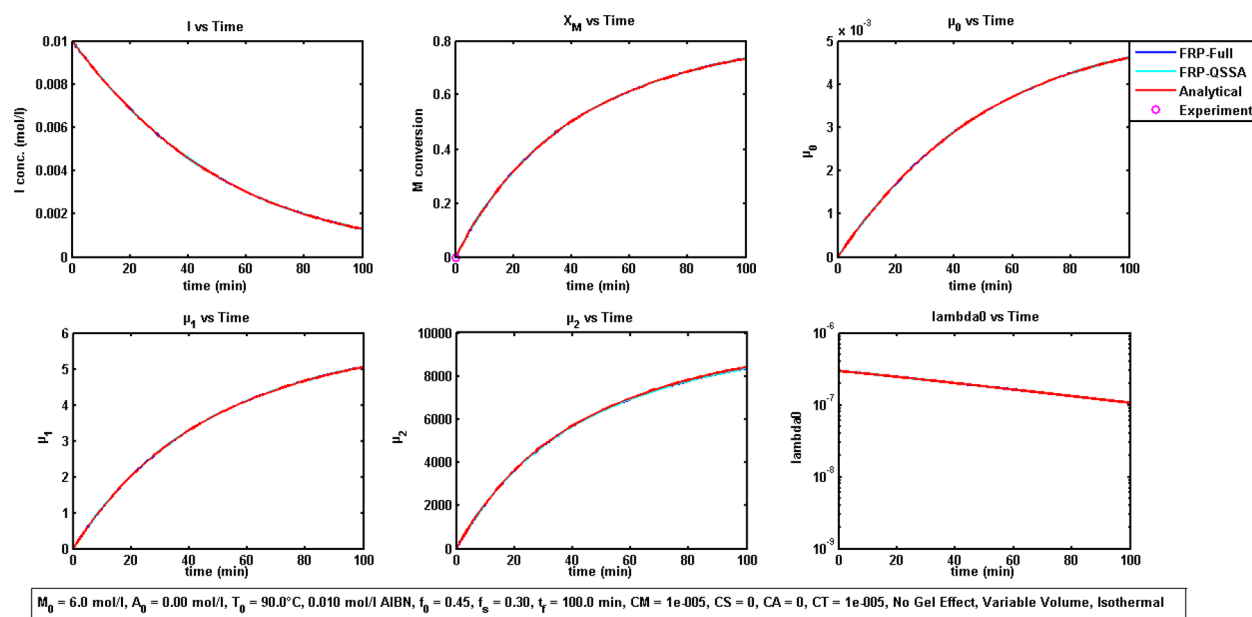


Figure 5. AS is compared for general case of isothermal solution polymerization with negligible transfer processes.

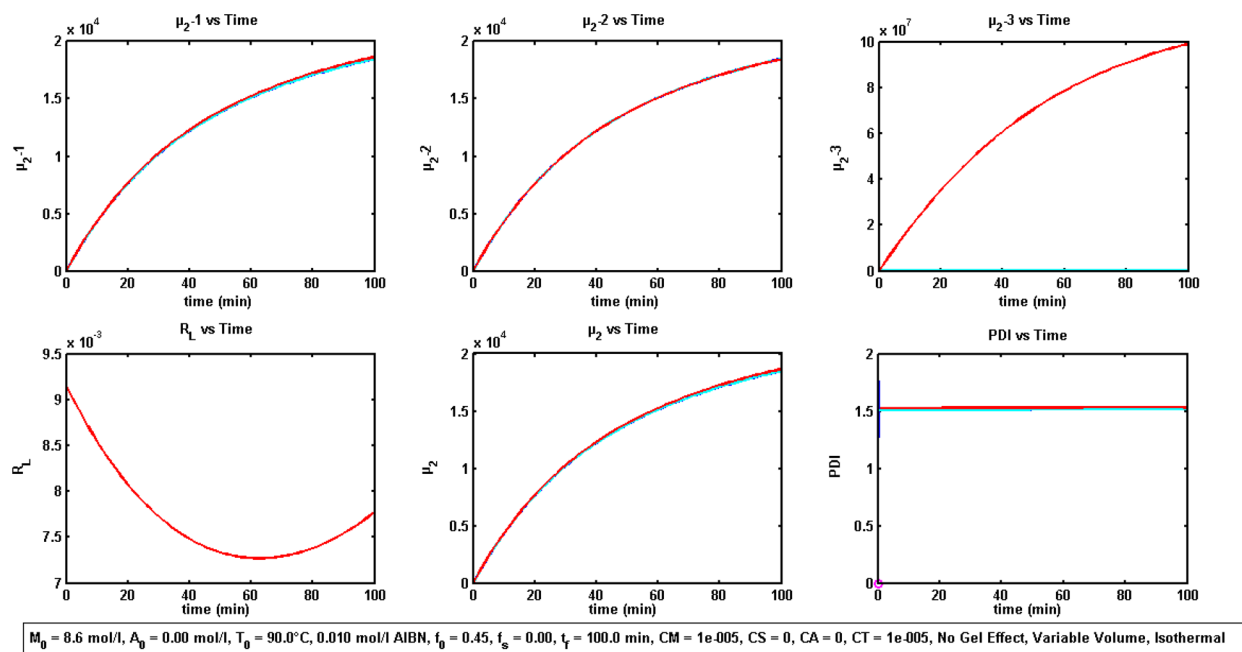


Figure 6. Case 1: $R_L < 0.1$, for general case of isothermal bulk polymerization with only transfer to monomer.

range of conversion. This proves also the observation that with increase in temperature, gel effect shifts to higher conversion and can be absent for higher temperature.

Figures 11 and 12 show the validation of AS with experimental data for solution polymerization for two different temperatures as well as two different solvent fractions. As can be seen, the results match well with conversion and PDI but exhibit some discrepancies when MW_n and MW_w are compared with experimental data. However, this is also the same for the numerical solution as well, and it still matches well with AS. The discrepancy observed for PDI results is due to small variation observed in MW_w values between AS and numerical solution as MW_n values match well in both AS and numerical solution. Thus, this variation arises due to the difference between the values of μ_2 returned by AS and numerical method. As we already know that

μ_2 solution consists of three cases and there is infinite series solution in first two cases. So in some cases, we can expect some numerical difference between AS and numerical solution for μ_2 value either due to insufficient/improper evaluation of infinite series solution and/or due to shifting of solution from one case to another.

Similar results and conclusions can be observed for MMA in Figures 13–15, where temperature varies from $T = 50^\circ\text{C}$ (a), 70°C (b), and 90°C (c). Again the match is good until the gel effect sets in. Here the match with MW_n , MW_w , and PDI is better compared to the case of styrene. One can also observe that the conversion at which gel effect occurs shifts to higher value with temperature as mentioned above.

Now we study the cases of BuA and VAc for which the reaction is much faster. Experimental data^{18,19} are available for solution

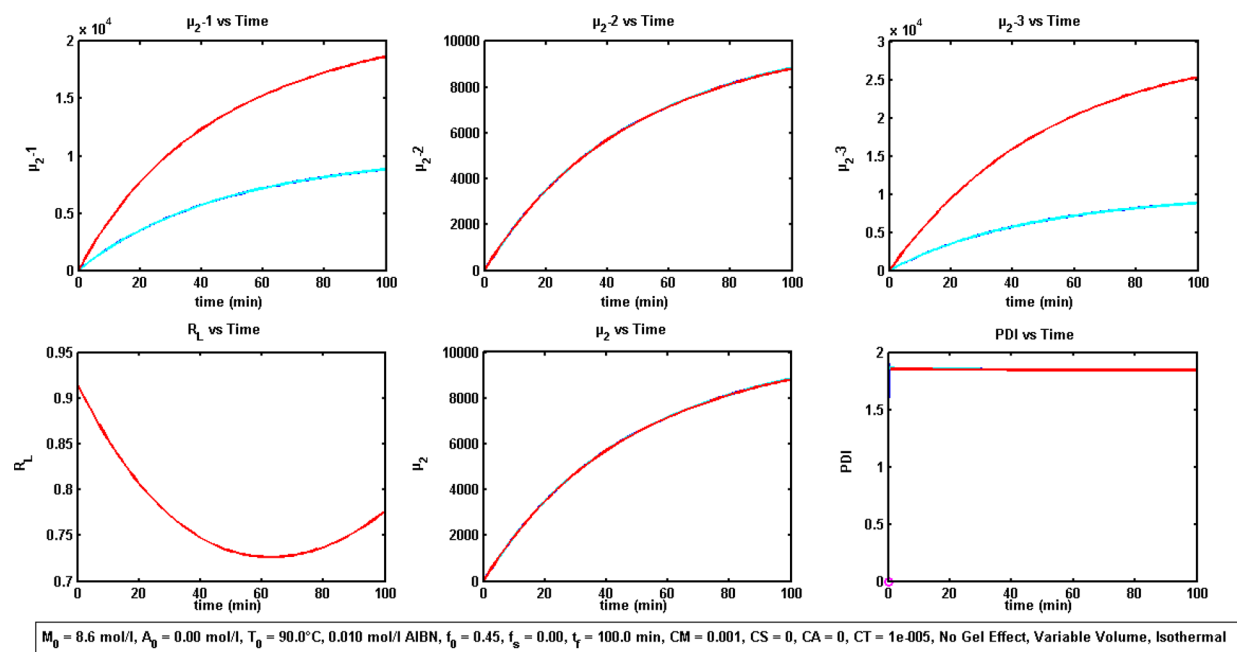


Figure 7. Case 2: $0.1 \leq R_L < 10$, for general case of isothermal bulk polymerization with only transfer to monomer.

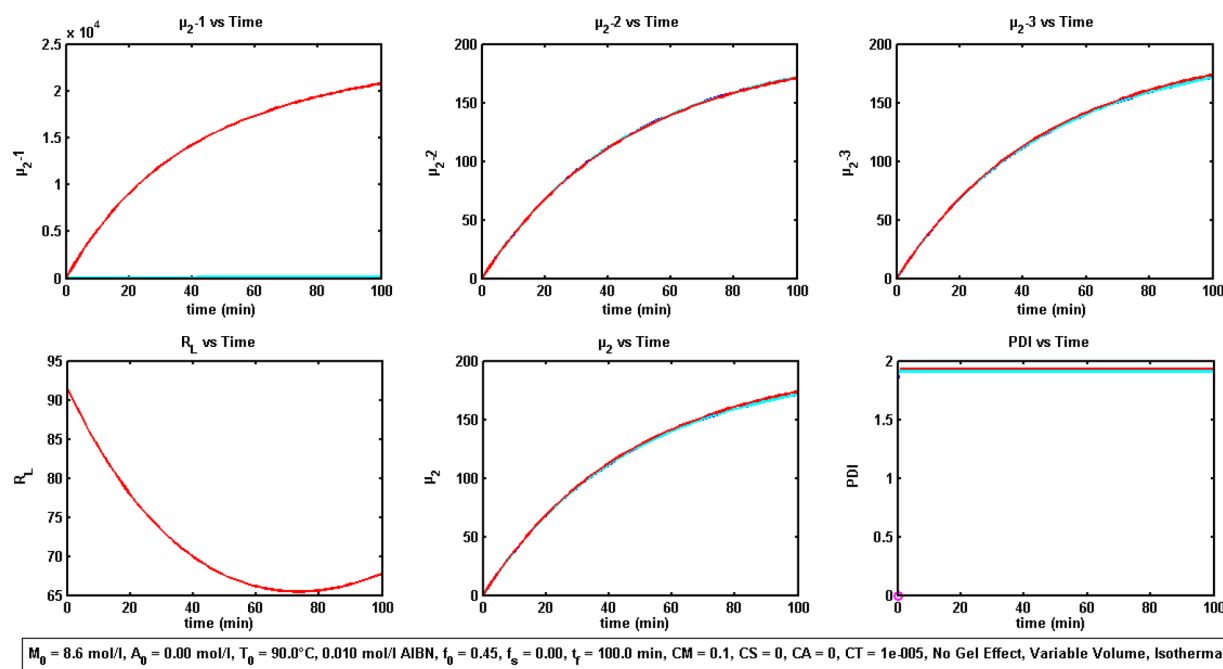


Figure 8. Case 3: $R_L \geq 10$, for general case of isothermal bulk polymerization with only transfer to monomer.

polymerization with different solvent volume fractions. Figures 16 and 17 consider two different temperatures with two different solvent fractions and common initiator AIBN; while Figure 18 addresses effect of another initiator (BPO) to demonstrate the versatility and generality of AS.

One can also observe that initiator efficiency exhibits quite low values and is a strong function of the solvent fraction. Similar observation has been reported by Verros and Achilias.¹⁴ This could possibly be due to large cage effect experienced by initiator at such a large solvent presence. This can change its efficiency even by small variation in solvent fraction. So, constant initiator efficiency could not be taken for all simulations as against the previous cases of St/PS and

MMA/PMMA and should be adapted to each operating condition. Therefore, the value of initiator efficiency is taken by matching the simulation results with experimental conversion data. The results match quite well for PDI although the prediction for MW_n is quite poor. The reason for this anomaly is unknown yet to us.

Similar results are visible for VAc through Figures 19 and 20, and same conclusions can be drawn.

DISCUSSION

From the above validation against numerical solution and confrontation with experimental data, many important comments can be made for the developed AS.

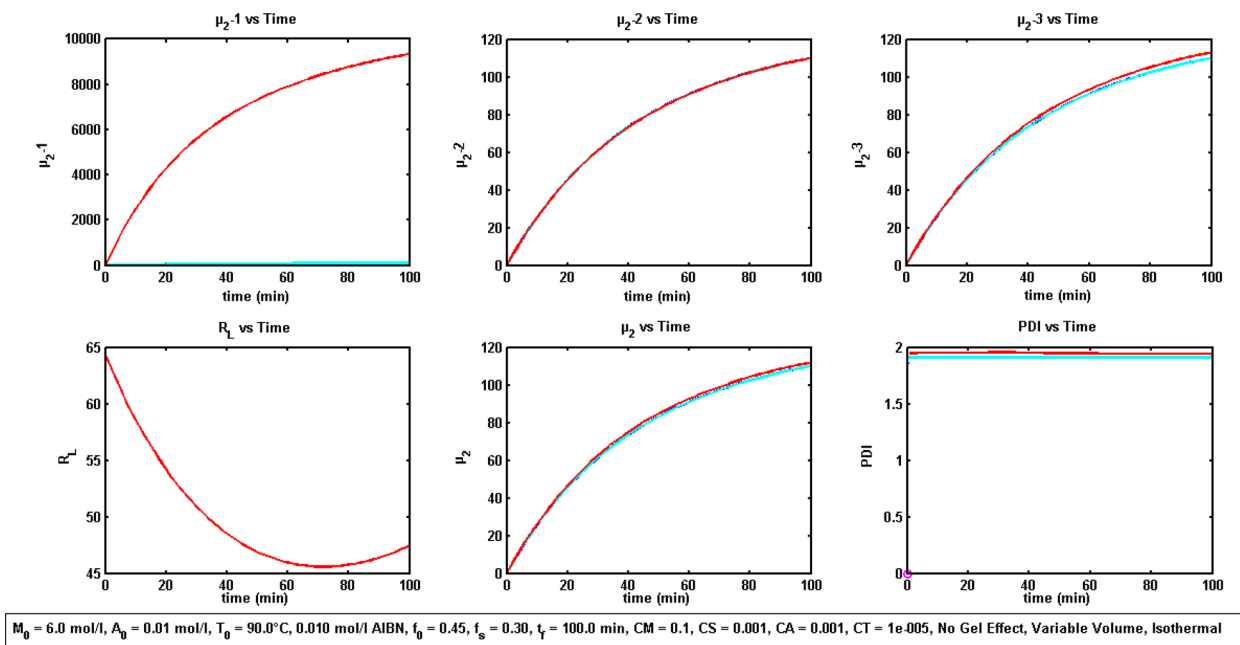


Figure 9. Case 3: $R_L \geq 10$, for general case of isothermal bulk polymerization with all transfer processes considered for the model, that is, C_M , C_S , and C_A .

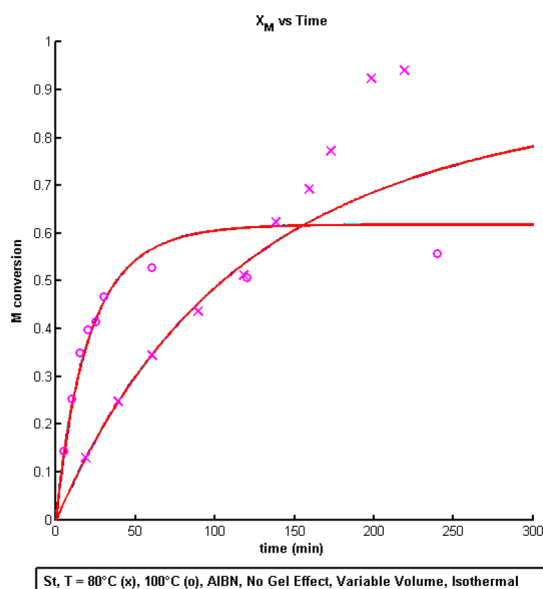


Figure 10. $St, T = 80^\circ\text{C}$ (x), 100°C (o), 0.5 mol/L AIBN (x), $T = 100^\circ\text{C}$, 0.0337 mol/L AIBN (o), $f = 0.45$.

μ_2 is found to be function of both R_L and R_T . No single solution exists, but rather three cases arise based on value of R_L . Recalling eq 45

$$R_L = R_p L$$

where R_p is given by eq A29

$$R_p = R_{MM} + R_{SM} + R_{AM} = \frac{C_M}{1 + C_M} + \frac{C_S}{1 + C_M} \frac{S}{M} + \frac{C_A}{1 + C_M} \frac{A}{M} = \frac{1}{1 + C_M} \left[C_M + C_S \frac{S}{M} + C_A \frac{A}{M} \right]$$

and L by eq 27

$$L = \frac{(K_p + K_{fm})M\lambda_0}{2fK_d I} = \frac{K_{pr}M\lambda_0}{2fK_d I}$$

Soh and Sundberg²⁵ have presented the four phases of vinyl polymerization of monomer soluble in its own polymer. The first phase represented the conventional kinetics, that is, the area of this work. The second phase represented the gel effect. The third phase was characterized by the slowing down of gel effect, and finally the fourth phase was identified by glass effect if the reaction temperature is less than the glass temperature of the polymer. Depending on the type of monomer used and/or the reaction conditions, one or more phases can be absent. The first phase according to the authors comes under conventional kinetics where the gel effect has not set in yet. It is same phase for which the AS was derived. They had characterized the last three phases by two important parameters (β_s and γ_s) and had obtained the results for the case of transfer to monomer and transfer to CTA. Comparing with the developed AS, we found that these two parameters also appeared in our solution as a function of R_p and L . They are as follows:

$$\frac{x_c}{\gamma_s \sqrt{Z_s}} = \frac{(1 - R_M)K_{pr}M\lambda_0}{2fK_d I} = (1 - R_M)L \quad (68)$$

$$\frac{\beta_s}{x_c} = \left[C_M + C_A \frac{A}{M} \right] = (1 + C_M)R_p \quad (69)$$

Recalling that both R_p and L defined R_L through eq 45 and that this last parameter described the phase 1 covered by our AS, it seems that the parameters of Soh and Sundberg²⁵ not only account for phases 2–4 of vinyl polymerization but should also characterize phase 1. Thus, the developed AS extends their result to the whole range of phases.

Zhu and Hamielec^{23,24} had defined the conditions under which gel formation could take place for isothermal, homogeneous, batch homopolymerization. The steps²⁴ considered were initiation, propagation, chain transfer to polymer, termination by combination and disproportionation, and chain transfer to monomer. The assumptions used for their work were (1) monoradical assumption, (2) stationary state hypothesis, and (3) random chain transfer to polymer. They found that gel formation

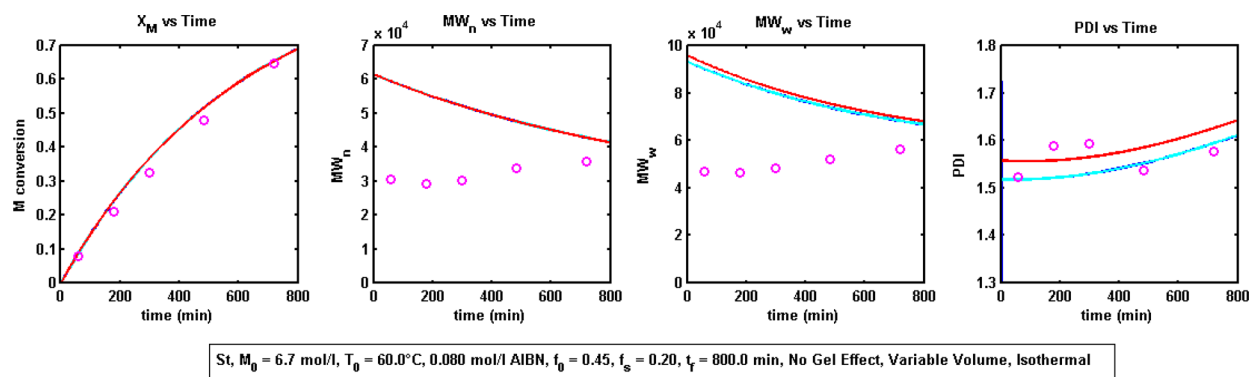


Figure 11. St^{16} data for solution polymerization at $T = 60^\circ\text{C}$, $f_s = 0.20$.

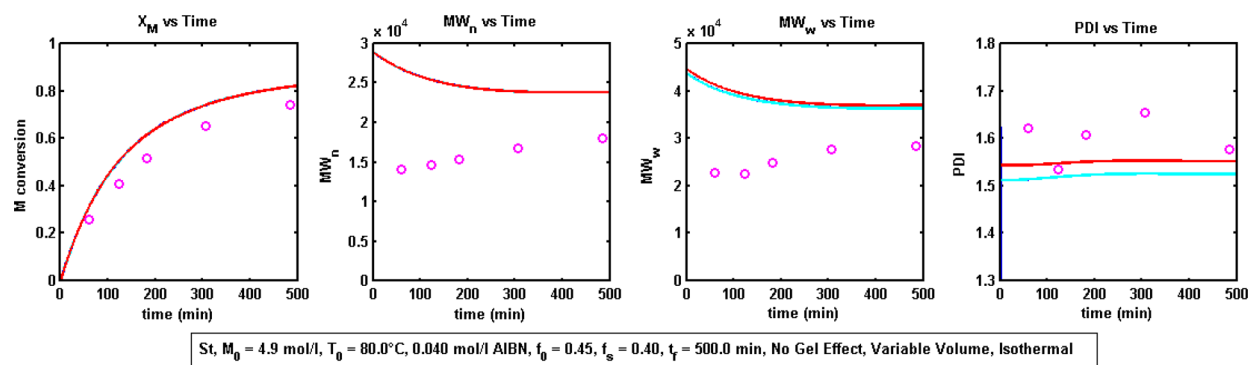


Figure 12. St^{16} data for solution polymerization at $T = 80^\circ\text{C}$, $f_s = 0.40$.

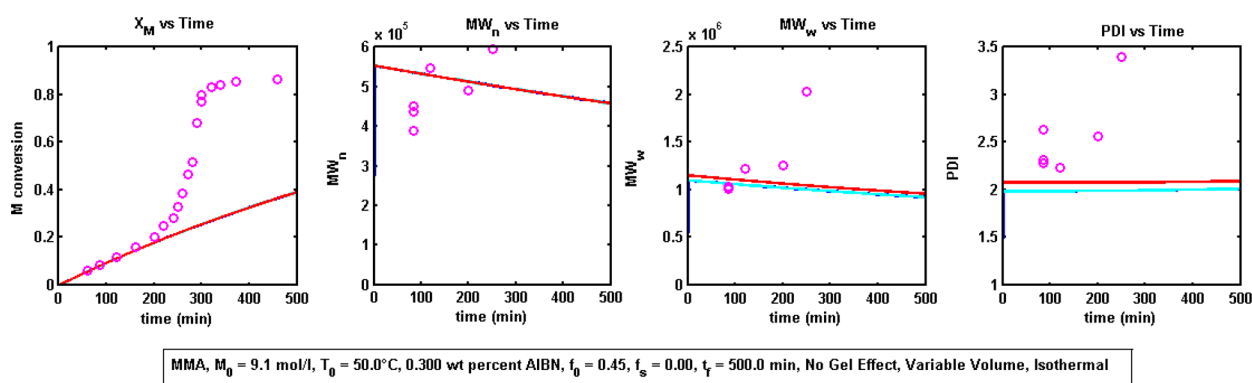


Figure 13. MMA^{17} for isothermal bulk polymerization at $T = 50^\circ\text{C}$.

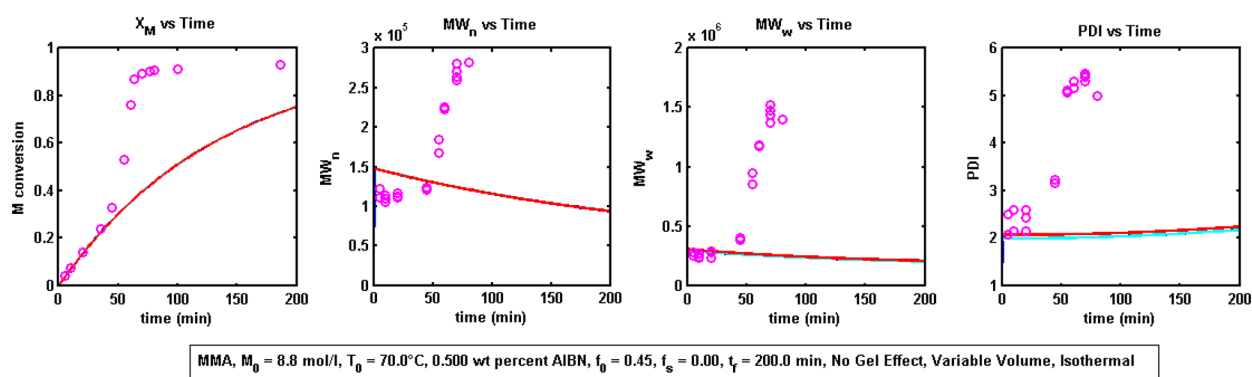


Figure 14. MMA^{17} for isothermal bulk polymerization at $T = 70^\circ\text{C}$.

in free radical polymerization could occur only through (1) transfer to polymer + termination by combination, (2) transfer to

polymer + termination by disproportionation, and (3) transfer to monomer + termination by recombination.

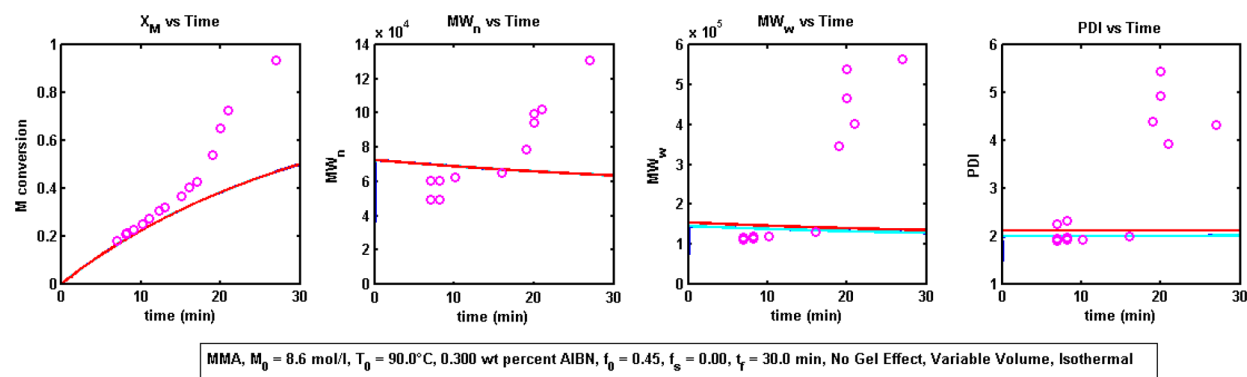


Figure 15. MMA¹⁷ for isothermal bulk polymerization at $T = 90^\circ\text{C}$.

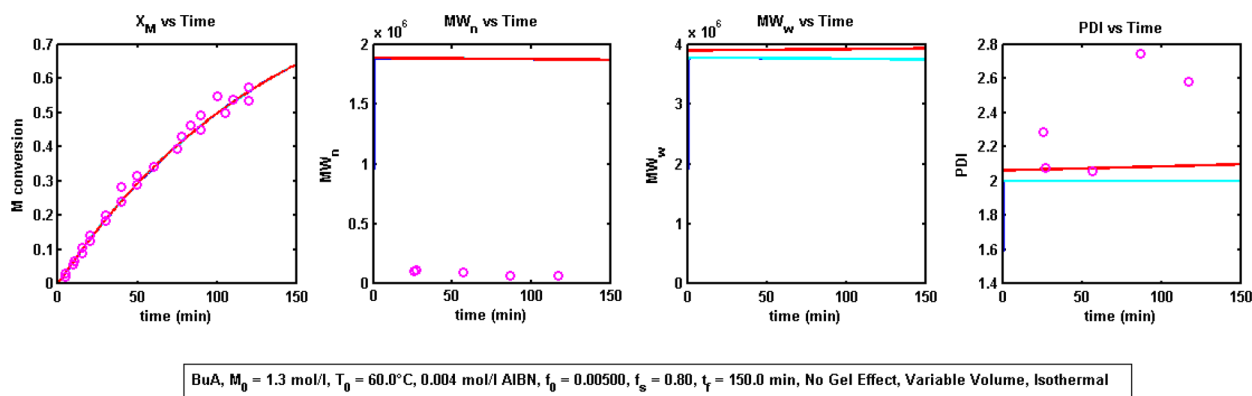


Figure 16. BuA¹⁸ for isothermal solution polymerization at $T = 60^\circ\text{C}$, AIBN.

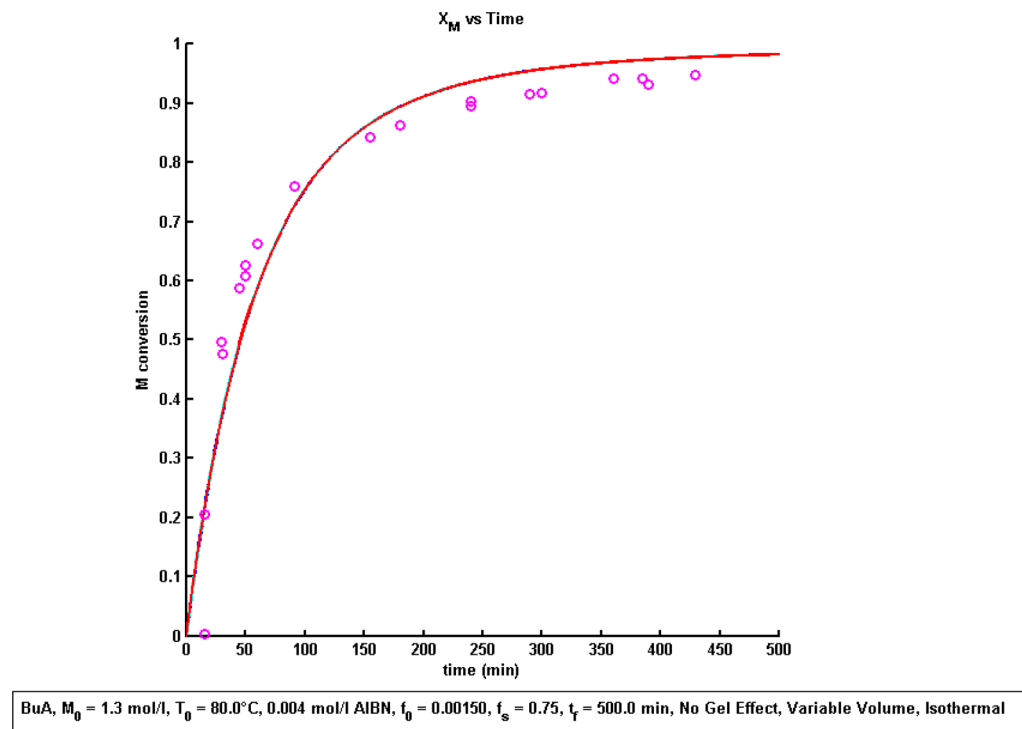


Figure 17. BuA¹⁸ for isothermal solution polymerization at $T = 80^\circ\text{C}$, AIBN.

They had shown that three factors ($(K_{fm}M_0)/(K_t\lambda_0)$, K_{tc}/K_t , and K_{p^*}/K_p) are of importance when the transfer to monomer led to gel effect. It is noteworthy that, for the presence of chain transfer to monomer ($C_M \neq 0$) and the absence of chain transfer

to solvent ($C_S = 0$) and CTA ($C_A = 0$), our R_L parameter is reduced to $(K_{fm}M)/(K_t\lambda_0)$, which is the Zhu and Hamielec²⁴ first parameter but at $t \neq 0$, that is, at any time t . The values of both would be the same at the beginning of the reaction. The second

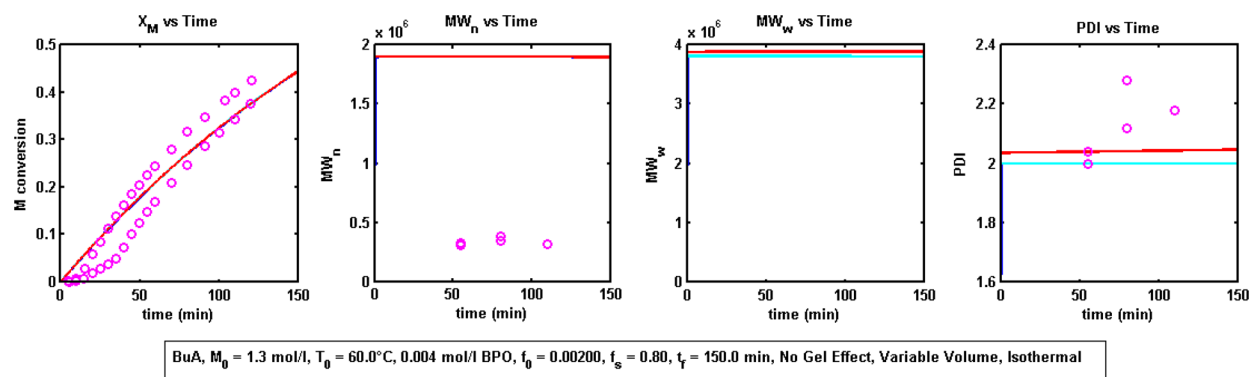


Figure 18. BuA¹⁸ for isothermal solution polymerization at $T = 60\text{ }^{\circ}\text{C}$, BPO.

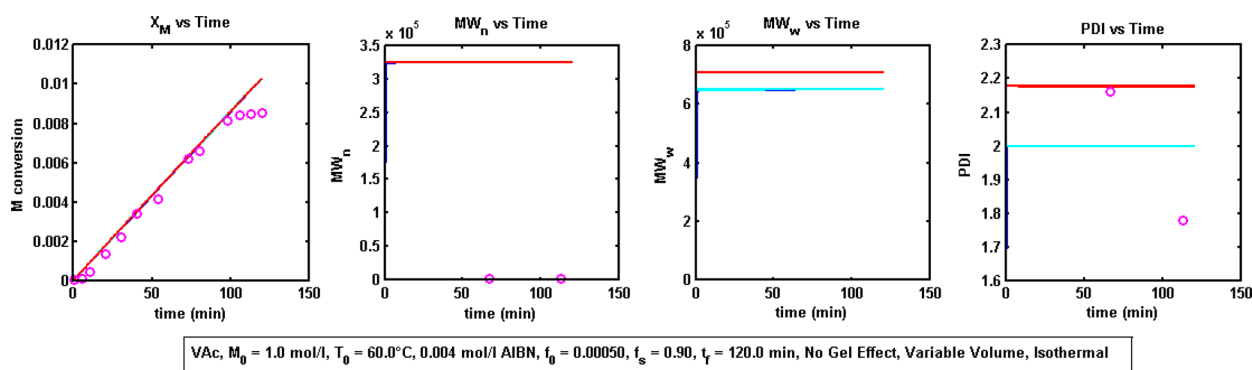


Figure 19. VAc¹⁹ for isothermal solution polymerization at $T = 60\text{ }^{\circ}\text{C}$, AIBN.

parameter is simply R_T , and the third is absent in our AS since we have not modeled K_p^* , the reaction rate coefficient for propagation for chain-end double bond. Authors²⁴ had shown that there was a combination of values between $(K_{tm}M_0)/(K_t\lambda_0)$ and K_{tc}/K_t (i.e., between R_L and R_T) below which the gel effect could not take place and that high value of $(K_{tm}M_0)/(K_t\lambda_0)$ did not always mean early gel point. This is quite apparent for the cases of BuA and VAc as shown in Figures 21 and 22. The value of R_L is definitely high, but there is no sign of gel effect as shown in their experimental conversion presented in Figures 18 and 20. This presents the beauty of AS which enables one to analyze such situations analytically. We have now observed the importance of the value of R_L in determining the direction of reaction toward the gel effect. Keeping this in mind, in our case, R_L is being evaluated at the beginning of each time step based on the information available at the beginning of that time step. This is particularly a good strategy as R_L can move from one case to another case as the reaction proceeds. So we can observe that, in certain cases, a monomer which may not be capable of moving into the gel phase based on the initial conditions alone may become capable of gel formation during the course of reaction and vice versa. Thus, this improves the methodology for predicting gel effect and its extent compared to the prediction based only on the initial conditions without updating them with the course of reaction as in the case of Zhu and Hamielec.²⁴

Although we have not taken the gel effect into account for the AS, it is worthy to note that a relation has emerged naturally between R_L and R_T in the AS. Indeed, we came up with three different cases for μ_2 , which seems to be in accordance with the observation made by Zhu and Hamielec²⁴ for predicting the capability for gel effect. This definitely establishes beyond any doubt that the AS is being evolved in a proper direction.

Besides this, the R_L parameter has a physical meaning too. It can easily be observed that it represents the ratio of primary radicals produced by consumption of live polymer chain radicals by chain transfer to monomer/CTA/solvent steps to primary radicals' production by initiator. It can also be viewed as the primary radicals' production by chain transfer processes compared to primary radicals produced by original initiator. So its value represents how strong is the chain transfer processes with respect to initiation process in terms of primary radicals' formation as well as termination of polymer chain radicals other than by termination steps. So its high value means that prolongation of polymer chain will be prevented earlier and the resulting chains will mostly be of small lengths. This will affect both MW_n and MW_w .

Our AS also matches with the expression of monomer concentration obtained by Venkateshwaran and Kumar⁹ under constant volume condition. Indeed, their solution is as follows:

$$M = M_0 e^{-m_v(Z_{0v}-Z_v)} \quad (70)$$

where

$$Z_v = 2\sqrt{\frac{2fk_tI_0 e^{(-k_d t)}}{k_d}} \quad (71)$$

$$Z_{0v} = 2\sqrt{\frac{2fk_tI_0}{k_d}} \text{ and } m_v = \frac{k_p}{k_t} \quad (72)$$

so

$$m_v Z_v = 2\sqrt{\frac{2fk_pI_0 e^{(-k_d t)}}{k_d k_t}} = B_0 y \quad (73)$$

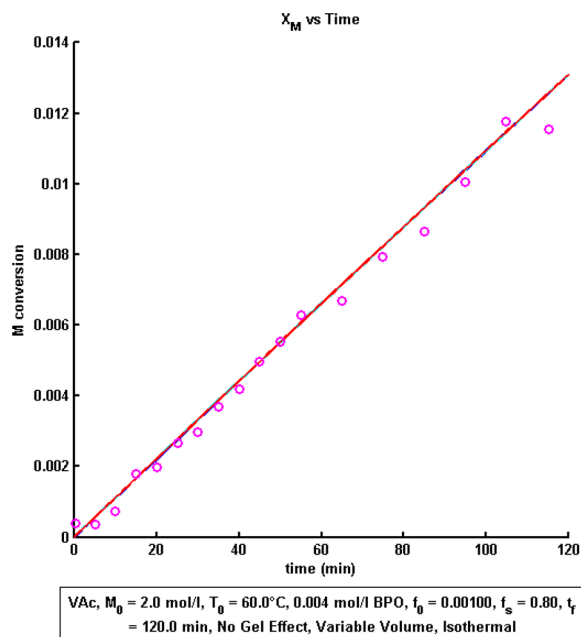


Figure 20. VAc¹⁹ for isothermal solution polymerization at $T = 60^\circ\text{C}$, BPO.

It is noteworthy that this last expression is same as the one shown in eqs 12 and 17. This means that, using this expression, one will end up with the same solution for monomer conversion as obtained in eq F3 (Appendix F, Supporting Information). So the solution obtained by the authors without using QSSA and ours using QSSA is the same. Except that we have obtained this solution in a much simpler way conversely to the authors who had applied several mathematical manipulations to reach this simple result. In a broad way, it can be concluded that the results obtained by following the model in its complexity by not applying QSSA is still the same when QSSA is applied. So this justifies the simplification obtained by this simple QSSA assumption.

Special attention is now directed toward the source of stiffness in FRP model. To get an idea of the time step size during which temperature change is so small that kinetic rate coefficients can be assumed to be constant, let us use the AS for M and λ_0 obtained so far. Recalling eqs 19, 32, and 67 we have

$$T' = e^{(K_1 t)} \int e^{(-K_1 t)} K_2 (1 - R_M) K_{pr} M_0 \cdot V_{R0} \times \exp[-B_0(1 - y)] \sqrt{\frac{2fK_d I}{K_t}} dt \quad (74)$$

Using eqs 11 and 12 for initiator concentration and y respectively, we obtain

$$T' = e^{(K_1 t)} \int e^{(-K_1 t)} K_2 (1 - R_M) K_{pr} M_0 \cdot V_{R0} \times \exp[-B_0(1 - y)] \sqrt{\frac{2fK_d I_0}{K_t} \cdot \frac{V_{R0}}{V_R}} e^{-K_d t/2} dt \quad (75)$$

As one can see, there are many expressions which contain exponential terms explicitly and others, like kinetic rate coefficients, in which these exponential terms are implicit. It will make the expression quite cumbersome if we put all the implicit exponential terms it contains. So let us just take the monomer term's exponential part and evaluate the temperature dependence.

$$\begin{aligned} \exp[-B_0(1 - y)] &= \exp(-B_0) \exp(B_0 y) \\ &= \exp(-B_0) \exp(B_0 e^{-K_d t/2}) \end{aligned} \quad (76)$$

$$\begin{aligned} &\exp(-B_0) \exp(B_0 e^{-K_d t/2}) \\ &= \exp(-B_0) \exp\left(B_0 \exp\left[-\frac{K_{d0} \exp\left[-\frac{E_{d0}}{RT}\right] t}{2}\right]\right) \end{aligned} \quad (77)$$

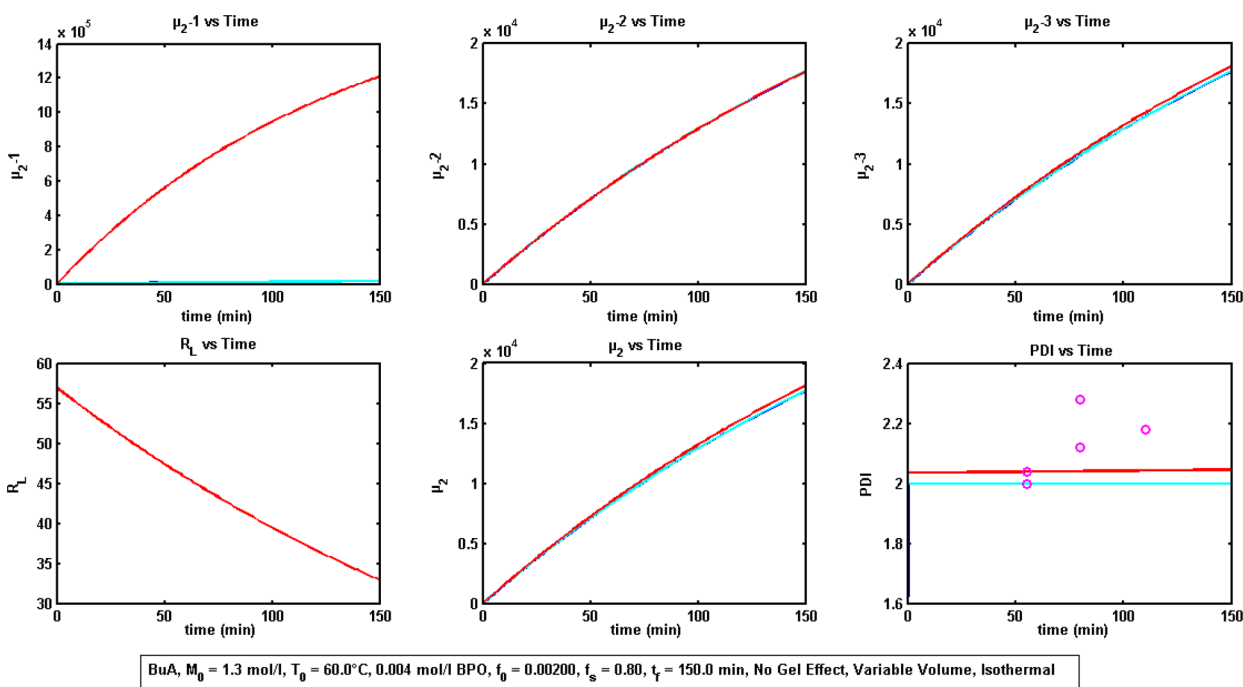


Figure 21. BuA,¹⁸ result for R_L .

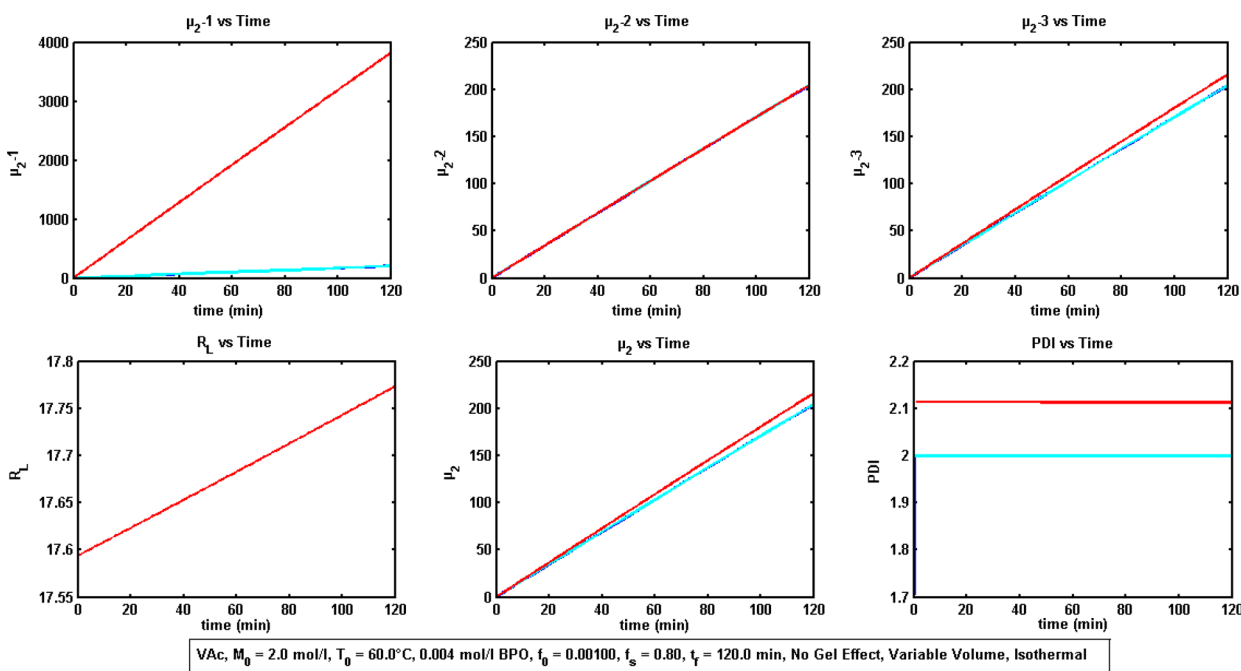


Figure 22. VAc, result for R_L .

$$= \exp(-B_0) \exp\left(B_0 \exp\left[-K_{d0} \frac{t}{2} \exp\left[-\frac{E_{d0}}{RT}\right]\right]\right) \quad (78)$$

So we can easily see that, with respect to temperature, the expression is thrice exponential. So even a small change in temperature will lead to large change in monomer conversion and heat generation, which ultimately can induce a thermal runaway. This is what happens in poorly controlled polymerization reactors. Thus, to keep the temperature change small enough, the time-step during which it is evaluated, should be very small. Depending on initial conditions, overall heat transfer coefficient (U), heat of reaction and thus time-step value may vary.

We can also observe that the expression is also dependent on time with twice exponential. As time can only increase and will lead to decrease of exponential function, thus heat generation can be delayed by increasing time of reaction, that is, by slowing down the reaction initially by keeping the temperature low and later speed up the reaction by increasing temperature. This seems to be practical, too. So instead of keeping an isothermal condition with one fixed temperature only for the whole conversion, the temperature can be increased after some suitable conversion to speed up the reaction rate. This could be done in steps or continuously. This is just a possibility we are suggesting based on our analysis and results. This may require separate study and/or reference to existing work^{27,28} as to how to calculate the “suitable conversion” and what should be best temperature profile.

We can observe from the AS and all presented graphs that there is no stiffness in this set of differential equations for the case of no gel effect, that is, eqs A1–A11. So from this, we can conclude that the only source of stiffness in this system of equations arises from temperature equation as previously discussed. So in the absence of this source, that is, for isothermal conditions, this model for FRP can easily be integrated using nonstiff solvers.

CONCLUSION

An analytical solution (AS) for FRP for variable volume, isothermal, homogeneous bulk/solution homopolymerization conditions is obtained. The solution for initiator and monomer already exists for constant volume case. For monomer, the same solution was obtained by Zhu and Hamielec.²¹ Venkateshwaran and Kumar⁹ had also obtained an AS, but their solution did not account for transfer to monomer and transfer to solvent. Besides this, the major disadvantage of their solution was that it was too cumbersome and complex, and hence almost impractical to choose for any purpose. Moreover, their AS matched poorly with numerical solution.

The solution we have obtained is quite elegant, simple, and noncumbersome. Under no gel effect condition or before gel effect, it can be easily implemented on any spreadsheet or programmable software. So the novelty of this work is to get an AS which is applicable not only for variable volume condition but also accommodates a large range of elementary steps that have practical usage in industry and lab alike.

The relationship of λ_0 , λ_1 , and λ_2 as shown by eqs 32–37 is also in accordance with the physical and theoretical reality which states that process of chain transfer like transfer to monomer, solvent and CTA should reduce the live or dead polymer chain length.

μ_0 , μ_1 , and μ_2 are shown to be dependent on both I_0 and M_0 . μ_0 and μ_1 are found to be simple functions of the final and initial concentration of initiator, monomer, solvent, and CTA. They are also independent of R_L .

It can be seen that the results of AS match quite well with numerical integration results for I , M , μ_0 , and μ_1 for all the cases. It matches quite well for μ_2 depending on the value of R_L to select the suitable case between three different possible cases. It is also observed that the results are quite sensitive toward the value of C_p rather than C_T . This implies that the side reaction of transfer processes like chain transfer to monomer has more impact on μ_2 and hence on PDI than the type of termination of reaction. It also signifies the importance of inclusion of the chain transfer to monomer for good modeling of FRP. Also assuming R_L as

variable constant for case 2 can be seen to be valid to a good extent as the variation in the value of R_L is generally quite small in that case. The procedure aiming at varying C_M value to match the AS of μ_2 with that of experimental data can be used to calculate the actual value of C_M at a given temperature. So one could estimate how much significant is the transfer to monomer process under operating conditions and derive some methods to reduce its importance in order to improve or control PDI.

It can also be seen that the results match quite well with the experimental data until the gel effect sets in. It is quite understandable as the assumption of constant reaction rate coefficients no longer remains valid after that. It can also be observed that the model based on QSSA, that is, FRP_QSSA, matches quite well with the full model, that is, FRP_Full. This is understandable as the condition of QSSA is violated only during the gel effect but not modeled here. Hence, the simplest model can be used in CFD, for instance, to model FRP in a given batch reactor or flow reactor geometry before the gel effect.

It could also be used for model based process control in the batch reactor during the production of polymer by FRP up to the conversion before gel effect (Sampath et al.²²).

Finally, this AS can be used to validate the numerical formulation in CFD or can be used in CFD simulations to calculate an initial condition value for individual cell instead of constant initial condition value for all cells as generally used. This can greatly reduce the simulation time required, as the initial solution will be close to the final solution from the very beginning of convergence procedure. For polymerization, using CFD, AS can also be used to evaluate the extent of mixing within the reactor with more precision without resorting to correlation technique.²⁶

The accuracy of prediction of AS is obviously limited by the accuracy of data especially the kinetic data used for the temperature range under study. So the range of applicability of data for that temperature must be verified before use.

It will be shown in a future paper that a simple modification in the algorithm can make the AS suitable to account for the gel effect, nonisothermal, and semibatch conditions.

■ ASSOCIATED CONTENT

● Supporting Information

Appendix A: Mathematical model of free radical polymerization used in this work. Appendix B: Derivation of monomer conversion. Appendix C: Derivation of μ_0 . Appendix D: Derivation of μ_1 . Appendix E: Derivation of μ_2 . Appendix F: Summary of analytical solution at any time t for constant volume condition. This material is available free of charge via the Internet at <http://pubs.acs.org>.

■ AUTHOR INFORMATION

Corresponding Author

*E-mail: ca.serra@unistra.fr (C.A.S.).

Notes

The authors declare no competing financial interest.

■ ACKNOWLEDGMENTS

The financial support by ANR Grant No. 09-CP2D-DIP² is greatly appreciated.

■ NOTATION

A = Chain transfer agent concentration at any time t , mol/L
 A_H = Area for heat transfer, m²
 $B_{n-1} = [(8f[K_{pr}]^2 I_{n-1}) / (K_d K_t)]^{1/2}$, constant in the AS at the beginning of $(n - 1)$ th time step

$C_A = K_{fa}/K_p$, dimensionless
 $C_M = K_{fm}/K_p$, dimensionless
 $C_{n-1} = 2B_{n-1}[(V_R/V_{R0})^{n-1}/(V_{R0})]^{1/2}$, constant in the AS at the beginning of $(n - 1)$ th time step
 C_p = Specific heat capacity of mixture, cal/g/°C
 $C_S = K_{fs}/K_p$, dimensionless
 $C_T = K_{td}/K_{tc}$, dimensionless
 $D_{n-1} = [(2(K_{pr}M_{n-1})^2)/(K_t K_d)]e^{-C_{n-1}}$, constant in the AS at the beginning of $(n - 1)$ th time step
 DP_n = Number-averaged degree of polymerization
 E_{d0} = Activation energy for dissociation rate constant, cal/mol
 I = Initiator concentration, mol/L
 $J_{n-1} = 4/R_p[(R_T/R_p)(1 + R_{SA}) + 1](\sqrt{K_t/K_d})[(2fK_d I_{n-1})^{3/2}/(K_{pr}M_{n-1})]$, constant in the AS at the beginning of $(n - 1)$ th time step
 $K1 = UA_H/\rho V_R C_p$, constant (s⁻¹)
 $K2 = (-\Delta H_p)/\rho V_R C_p$, constant (°C/mol)
 K_d = Dissociation rate coefficient, min⁻¹
 K_{d0} = Pre-exponential factor of K_d , dissociation rate coefficient, min⁻¹
 K_{fa} = Transfer to CTA rate coefficient, l/(mol·min)
 K_{fm} = Transfer to monomer rate coefficient, l/(mol·min)
 K_{fs} = Transfer to solvent rate coefficient, l/(mol·min)
 K_p = Propagation rate coefficient, l/(mol·min)
 $K_{pr} = K_p + K_{fm} = (1 + C_M)K_p$, l/(mol·min)
 $K_t = K_{tc} + K_{td}$, l/(mol·min)
 K_{tc} = Termination by combination rate coefficient, l/(mol·min)
 K_{td} = Termination by disproportionation rate coefficient, l/(mol·min)
 L = Kinetic chain length, $(K_{pr}M_0)/(2fK_d I)$
 $\bar{L} = L[(1 - R_{MM})/(1 + R_p L)] = L[(1 - R_M)/(1 + R_p L)]$
 M = Monomer concentration, mol/L
 MW_M = Molecular weight of monomer, g/mol
 MW_n = Number-averaged chain length of polymer, g/mol
 MW_w = Weight-averaged chain length of polymer, g/mol
 $P = (2/(R_L + 1)) + R_T/(R_L + 1)^2$, parameter in the AS
 PDI = Polydispersity index, dimensionless
 P_n = Dead polymer chain length of n no. of monomer units
 $Q_{n-1} = (2R_T/R_p^2)(K_t/K_d)[(2fK_d I_0)^2/(K_{pr}M_n)^2]$, constant in the AS at the beginning of $(n - 1)$ th time step
 R = Universal gas constant, 1.986 cal/mol/K
 R_0 = Zero order radical obtained from initiator dissociation
 $R_A = C_A/(1 + C_M) = K_{fa}/K_{pr}$
 $R_{AM} = C_A/(1 + C_M)(A/M) \approx C_A/(1 + C_M)(A_0/M_0)$
 $R_L = R_p L$, parameter in the AS
 $R_M = K_{fm}/(K_p + K_{fm}) = K_{fm}/K_{pr} = C_M/(1 + C_M)$
 $R_{MM} = R_M$
 R_n = Live polymer chain length of n no. of monomer units
 $R_p = R_{MM} + R_{SM} + R_{AM} = R_{MM} + R_{SA}$
 $R_S = C_S/(1 + C_M) = K_{fs}/K_{pr}$
 $R_{SA} = R_{SM} + R_{AM}$
 $R_{SM} = C_S/(1 + C_M)(S/M) \approx C_S/(1 + C_M)(S_0/M_0)$
 $R_T = K_{tc}/(K_{tc} + K_{td}) = K_{tc}/K_t = 1/(1 + C_T)$, dimensionless
 S = Solvent concentration any time t , mol/L
 T = Temperature, K
 $T' = T - T_{bath}$
 T_{bath} = Temperature of heat sink, K
 U = Overall heat transfer coefficient, W/m²/K
 V_R = Volume of solution at any time t , L
 V_{R0} = Initial volume of solution at t_0 , L
 Z_v, Z_{ov} = Parameter used by Venkateshwaran and Kumar⁹
 f = Initiator efficiency, dimensionless

f_s = Solvent volume fraction, dimensionless
 m_v = Parameter used by Venkateshwaran and Kumar⁹
 t = Time, min
 x_M = Monomer conversion, dimensionless
 $y = e^{(-K_d t)/2}$, variable evaluated in the AS
 ΔH_p = Heat of reaction, cal/mol
 β = Ratio of solvent volume to nonsolvent volume, dimensionless
 x_c = Physical constant of the polymer as used by Soh and Sundberg²⁵
 γ_s, β_s, Z_s = Parameters specified by Soh and Sundberg²⁵
 ε = Volume contraction factor corrected for solvent volume fraction, dimensionless
 ε_0 = Volume contraction factor without solvent volume fraction, dimensionless
 λ_0 = Zeroth order moment for live polymer chain length distribution, mol/L
 λ_1 = First order moment for live polymer chain length distribution, mol/L
 λ_2 = Second order moment for live polymer chain length distribution, mol/L
 μ_0 = Zeroth order moment for dead polymer chain length distribution, mol/L
 μ_1 = First order moment for dead polymer chain length distribution, mol/L
 μ_2 = Second order moment for dead polymer chain length distribution, mol/L
 ρ = Mixture density, g/cm³
 ϕ = Volume fraction, dimensionless

Subscript

M = Monomer
 P = Polymer
 S = Solvent
 I = Initiator
 n = At the beginning of n th time step

REFERENCES

- (1) Tulig, T. J.; Tirrell, M. Toward a Molecular Theory of the Trommsdorff Effect. *Macromolecules* **1981**, *14* (5), 1501–1511.
- (2) Chiu, W. Y.; Carratt, G. M.; Soong, D. S. A Computer-Model for the Gel Effect in Free-Radical Polymerization. *Macromolecules* **1983**, *16* (3), 348–357.
- (3) Baillagou, P. E.; Soong, D. S. Major Factors Contributing to the Nonlinear Kinetics of Free-Radical Polymerization. *Chem. Eng. Sci.* **1985**, *40* (1), 75–86.
- (4) Louie, B. M.; Carratt, G. M.; Soong, D. S. Modeling the Free-Radical Solution and Bulk-Polymerization of Methyl-Methacrylate. *J. Appl. Polym. Sci.* **1985**, *30* (10), 3985–4012.
- (5) Tefera, N.; Weickert, G.; Westerterp, K. R. Modeling of free radical polymerization up to high conversion. I. A method for the selection of models by simultaneous parameter estimation. *J. Appl. Polym. Sci.* **1997**, *63* (12), 1649–1661.
- (6) Tefera, N.; Weickert, G.; Westerterp, K. R. Modeling of free radical polymerization up to high conversion. II. Development of a mathematical model. *J. Appl. Polym. Sci.* **1997**, *63* (12), 1663–1680.
- (7) Frounchi, M.; Farhadi, F.; Mohammadi, R. P. Simulation of Styrene Radical Polymerisation in Batch Reactor- A Modified Kinetic Model for High Conversion. *Sci. Iran.* **2002**, *9* (1), 86–92.
- (8) Achilias, D.; Kiparissides, C. Modeling of Diffusion-Controlled Free-Radical Polymerization Reactions. *J. Appl. Polym. Sci.* **1988**, *35* (5), 1303–1323.
- (9) Venkateshwaran, G.; Kumar, A. Solution of Free-Radical Polymerization. *J. Appl. Polym. Sci.* **1992**, *45* (2), 187–215.
- (10) Achilias, D. S. A review of modeling of diffusion controlled polymerization reactions. *Macromol. Theory Simul.* **2007**, *16* (4), 319–347.
- (11) Achilias, D. S.; Kiparissides, C. Development of a General Mathematical Framework for Modeling Diffusion-Controlled Free-Radical Polymerization Reactions. *Macromolecules* **1992**, *25* (14), 3739–3750.
- (12) Keramopoulos, A.; Kiparissides, C. Development of a comprehensive model for diffusion-controlled free-radical copolymerization reactions. *Macromolecules* **2002**, *35* (10), 4155–4166.
- (13) Keramopoulos, A.; Kiparissides, C. Mathematical Modeling of diffusion-controlled free-radical terpolymerization reactions. *J. Appl. Polym. Sci.* **2003**, *88* (1), 161–176.
- (14) Verros, G. D.; Achilias, D. S. Modeling Gel Effect in Branched Polymer Systems: Free-Radical Solution Homopolymerization of Vinyl Acetate. *J. Appl. Polym. Sci.* **2009**, *111* (5), 2171–2185.
- (15) Wu, J. Y.; Shan, G. R. Kinetic and molecular weight control for methyl methacrylate semi-batch polymerization. I. Modelling. *J. Appl. Polym. Sci.* **2006**, *100* (4), 2838–2846.
- (16) Marten, F. L.; Hamielec, A. E. High-Conversion Diffusion-Controlled Polymerization of Styrene. I. *J. Appl. Polym. Sci.* **1982**, *27* (2), 489–505.
- (17) Balke, S. T.; Hamielec, A. E. Bulk Polymerization of Methyl Methacrylate. *J. Appl. Polym. Sci.* **1973**, *17*, 905–949.
- (18) McKenna, T. F.; Villanueva, A.; Santos, A. M. Effect of solvent on the rate constants in solution polymerization. Part I. Butyl acrylate. *J. Polym. Sci., Polym. Chem.* **1999**, *37* (5), 571–588.
- (19) McKenna, T. F.; Villanueva, A. Effect of solvent on the rate constants in solution polymerization. Part II. Vinyl acetate. *J. Polym. Sci., Polym. Chem.* **1999**, *37* (5), 589–601.
- (20) Baillagou, P. E.; Soong, D. S. Molecular-Weight Distribution of Products of Free-Radical Non-Isothermal Polymerization with Gel Effect - Simulation for Polymerization of Poly(Methyl Methacrylate). *Chem. Eng. Sci.* **1985**, *40* (1), 87–104.
- (21) Zhu, S.; Hamielec, A. E. Polymerization Kinetic Modeling and Macromolecular Reaction Engineering. In *Polymer Science: A Comprehensive Reference*; Matyjaszewski, K., Möller, M., Eds.; Elsevier B.V.: Amsterdam, 2012; Vol. 4, p 779–831.
- (22) Sampath, V.; Palanki, S.; Cockburn, J. C. Robust nonlinear control of polymethylmethacrylate production in a batch reactor. *Comput. Chem. Eng.* **1998**, *22*, S451–S457.
- (23) Zhu, S.; Hamielec, A. E. Modeling of Free-Radical Polymerization with Cross-Linking - Monoradical Assumption and Stationary-State Hypothesis. *Macromolecules* **1993**, *26* (12), 3131–3136.
- (24) Zhu, S.; Hamielec, A. E. Gel Formation in Free-Radical Polymerization Via Chain Transfer and Terminal Branching. *J. Polym. Sci., Polym. Phys.* **1994**, *32* (5), 929–943.
- (25) Soh, S. K.; Sundberg, D. C. Diffusion-Controlled Vinyl Polymerization. I. The Gel Effect. *J. Polym. Sci., Polym. Chem.* **1982**, *20* (5), 1299–1313.
- (26) Bothe, D. Evaluating the Quality of a Mixture; Degree of Homogeneity and Scale of Segregation. In *Micro and Macro Mixing: Analysis, Simulation and Numerical Calculation*; Bockhorn, H., Mewes, D., Peukert, W., Warnecke, H.-J., Eds.; Springer-Verlag: Berlin, 2010;.
- (27) Ray, A. B.; Saraf, D. N.; Gupta, S. K. Free-Radical Polymerizations Associated with the Trommsdorff Effect under Semibatch Reactor Conditions. I: Modeling. *Polym. Eng. Sci.* **1995**, *35* (16), 1290–1299.
- (28) Srinivas, T.; Sivakumar, S.; Gupta, S. K.; Saraf, D. N. Free radical polymerizations associated with the Trommsdorff effect under semi-batch reactor conditions. II: Experimental responses to step changes in temperature. *Polym. Eng. Sci.* **1996**, *36* (3), 311–321.